# EPSTEIN-BARR VIRUS AND THE CELLULAR DNA DAMAGE RESPONSE

by

Nenad Sejic

A thesis submitted to the University of Birmingham for the degree of

**MRes Cancer Sciences**

Supervisors: Dr Claire Shannon-Lowe, Dr Roger Grand

School of Cancer Sciences
College of Medical and Dental Sciences
University of Birmingham
August 2014

## ABSTRACT

EBV is an oncogenic human gammaherpesvirus which infects B lymphocytes and epithelial cells. New virus replication occurs in both cell types and EBV encodes proteins to replicate its own DNA. Selective activation of the DNA damage response (DDR) is thought to occur in order for the virus to efficiently conserve its DNA sequence. Components of the double strand break homologous repair pathway are known to be recruited to viral replication compartments and loaded onto viral DNA to achieve efficient and faithful replication of the viral DNA.

Using an epithelial cell line latently infected with EBV, we demonstrated interactions between the phosphorylated replication protein A (RPA) and the viral lytic proteins BALF2 (DNA binding protein) and BMRF1 (polymerase accessory factor). However, despite its presence at replication centres, we failed to identify its direct interaction with the viral proteins by co-immunoprecipitation and mass spectrometry. Analysis of viral gene expression after ATM inhibition suggests that ATM does not promote the expression EBV lytic genes and is perhaps inhibitory. However, we did identify a novel interaction between BALF2 and the mitochondrial $H^{+}$-$Ca^{2+}$ exchanger LETM1, suggesting a new role for BALF2 possibly in inhibition of apoptosis during the viral lytic cycle.

## ACKNOWLEDGEMENTS

I would like to take this opportunity to thank all those who have helped me throughout this research project. I would like to express my gratitude to Dr Claire Shannon-Lowe for her guidance and inspiration throughout this year. I would also like to give special thanks to Dr Roger Grand for his support during my development as a young scientist.

Discussions and technical support from Dr Rosemary Tierney and Robert Hollingworth proved to be invaluable in the generation of this thesis. I would also like to thank the B cell group and the many EBV investigators here in Cancer Sciences for their encouragement and interest towards my work.

## TABLE OF CONTENTS

# INTRODUCTION

## 1.1 EBV life cycle

Epstein-Barr virus (EBV) is a γ-herpesvirus carried by more than 90% of the world population (Rickinson and Kieff, 2001). The majority of carriers are infected asymptomatically during childhood; however, the virus is associated with infectious mononucleosis in adulthood. As with all herpesviruses, EBV persists for the entire lifetime of the host and it does this as a latent infection of memory B lymphocytes (Babcock et al, 1998). Here, viral gene expression is down-regulated to only the non-coding RNAs, EBERs and BARTs, (known as latency 0) in order to evade immune detection (Rickinson and Kieff, 2001). It is thought that the virus passes from person to person by the exchange of saliva followed by direct entry into tonsillar B cells. The interaction between the viral gp350 protein and the B cell surface molecule CD21 is fundamental in the entry process for the virus (Nemerow et al, 1987). The virus also has the potential to enter epithelial cells by co-transfer infection with EBV coated B cells. Direct infection of epithelial cells is probably not a naturally occurring event due to the lack of CD21 expression at the cell's surface (Shannon-Lowe et al, 2011). To replicate, the virus must enter its lytic cycle where it expresses most of its genome in order to generate new virus particles. This is seen *in vivo* when EBV carrying memory B cells differentiate into plasma cells (Laichalk et al, 2005) and during the differentiation of primary keratinocytes (Fedeerle et al, 2007).

## 1.2 EBV associated malignancies and latency patterns

EBV is associated with many lymphomas and epithelial malignancies of various origins. The virus was first identified in the UK in 1964 by analysis of Burkitt's Lymphoma samples imported from sub-Saharan

Africa (Epstein et al, 1964). Burkitt's lymphoma, with the endemic form being EBV associated, is a B cell carcinoma that is characterised by the presence of a c-Myc translocation which is likely to be responsible for the increased proliferation (Taub et al, 1982). Hodgkin's lymphoma (HL) and extranodal NK/T cell lymphoma (ENKTL) are also known to be EBV associated to varying degrees. It has also been shown that EBV contributes to the pathogenesis of the epithelial malignancies nasopharyngeal carcinoma (NPC) and gastric carcinoma (GC) (Thompson and Kurzrock, 2004). In the immunocompromised host, there are also occurrences of EBV-associated post-transplant lymphoproliferative disease (PTLD). The contribution of the virus towards these conditions is difficult to confirm, but it is thought that proteins encoded by latent genes contribute to the cancer cell phenotype.

EBV has a distinct pattern of gene expression depending upon the type of malignancy. The key latency genes are the nuclear antigen genes (EBNA-1, EBNA-2, EBNA-3 (A, B and C), EBNA-LP), the latent membrane proteins (LMP1, LMP2A, LMP2B) and the previously mentioned non coding RNAs (EBERs and BARTs). In various combinations, they form the latency patterns latency 0, latency 1, latency 2 or latency 3 (Thompson and Kurzrock, 2004) as shown in **figure 1.1**.

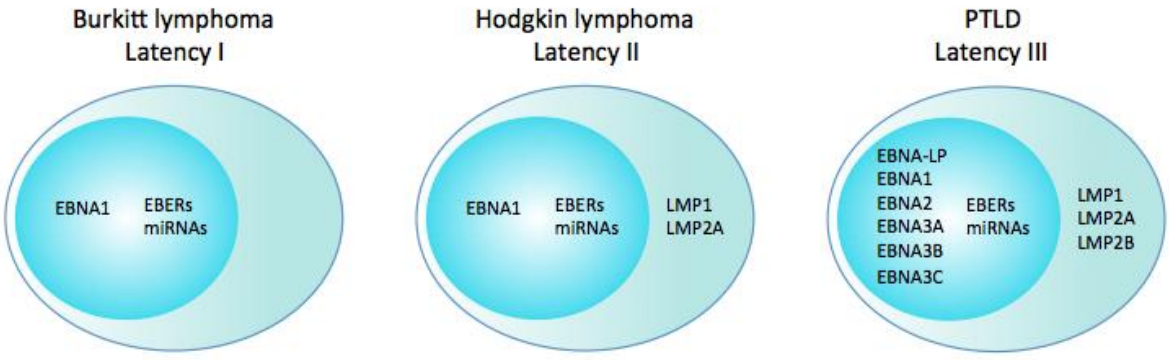


**Figure 1.1 EBV latency phenotypes of the different B cell malignancies associated with EBV.** EBV encodes different combinations of latency-associated genes depending upon the malignancy. (Diagram courtesy of C. Shannon-Lowe).

## 1.3 EBV lytic cycle

Lytic cycle is where the virus replicates its DNA and forms new virions before the lysis of the host cells and the release of infectious particles into the surrounding environment. To do this, the virus must express its lytic genes which are subcategorised based on the sequence of their expression: immediate early, early and late genes (**figure 1.2**). The key event in the latent to lytic switch is the expression of the immediate early gene BZLF1. BZLF1 acts as a transcription factor and has binding sites at the promoters of lytic gene waiting to be transcribed (Rooney et al, 1989). The other immediate early gene, BRLF1, also acts as a transcriptional activator with each of the pair contributing to the other's expression (Liu and Speck, 2003). Major components of the 30+ early genes are: BALF5 (DNA polymerase), BMRF1 (polymerase accessory protein), BALF2 (DNA binding protein), BMLF1 (mRNA export factor), BHRF1 (Bcl-2 homologue) and BGLF4 (protein kinase). BMRF1, BALF2 and BALF5 are known to locate to replication compartments within the nucleus of the host cell along with the immediate early proteins. Viral DNA is replicated as large concatameric molecules which are later cleaved to produce genomes of roughly 170kb which are packaged within capsid proteins encoded by the late genes (Daikoku et al, 2005).

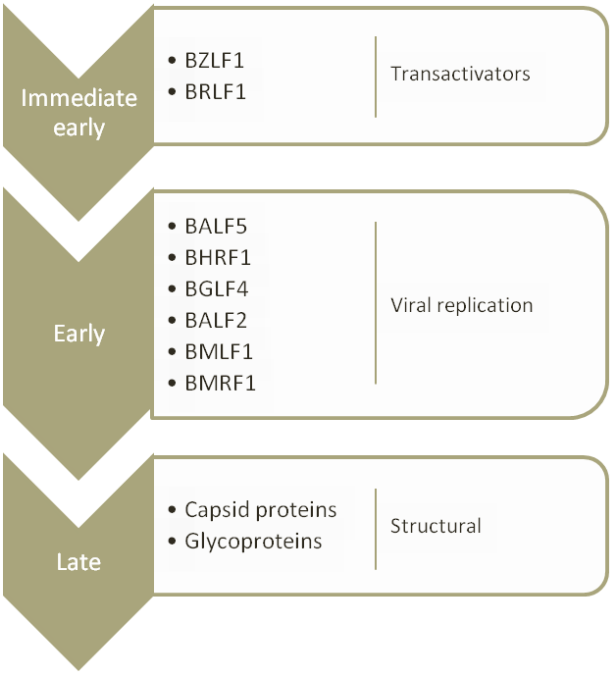


**Figure 1.2 Summary of EBV genes expressed in lytic cycle.** Immediate early genes BZLF1 and BRFL1 are expressed first then induce each others expression and the expression of the other lytic genes. Early genes are subsequently expressed and are involved in the replication of viral DNA and modulating the host cell. This is followed by the expression of late genes encoding capsid and glycoproteins for viral DNA packaging.

## 1.4 EBV and the host

EBV encodes proteins which enhance its survival my modulating cellular conditions within the host cell. During latency, EBNA-2 and EBNA-LP work together to drive the cell into the G1 phase of the cell cycle by binding p53 protein (Szekely et al, 1993). LMP1 is capable of mimicking CD40 at the B cell surface therefore resulting in greater cell growth (Zimber-Strobl et al, 1996). The viral BCRF1 gene encodes an IL10 homolog which acts as an immunosuppressive cytokine that deters the action of T lymphocytes and macrophages which would be clearly advantageous to the occupying virus (Slobedman et al, 2009). There is also evidence that EBV has some effect on the cell during its lytic cycle. One cellular aspect that is currently under intense investigation is EBV's relationship with the DNA damage response.

## 1.5 Cellular DNA damage

Individual cells are subject to tens of thousands of DNA damage lesions in any given day. These lesions may be induced by either endogenous or exogenous factors. Endogenous factors include DNA mismatches from ordinary replication or strand breaks that arise from topoisomerase errors (Jackson and Bartek, 2009). Reactive oxygen species (ROS) are a product of oxidative respiration and can induce chromosomal instability. ROS are also deployed by cells of the innate immune system as a mechanism of defence against infection (Kawanishi et al, 2006). ROS can impair DNA replication and induce base loss and single strand breaks (SSBs). When two SSBs are in close proximity, they may form the more toxic type of DNA damage, a double strand break (DSB). Exogenous inducers of DNA damage include UV light and ionising radiation. Ionising gamma radiation (e.g. from medical diagnostics from X-rays) can induce various forms of DNA damage including DSBs (Ward, 1990).

## 1.6 The DNA damage response

The DNA damage response (DDR) is a network of signalling pathways which have evolved to repair such breaks described above and preserve genome sequences to pass on to daughter cells. Members of the DDR can be divided into 4 major categories: DNA damage sensors, signal mediators, signal transducers and effectors. The effectors elicit the cellular response which is essentially either DNA damage repair or cell death. Dependent upon the type of damage sustained, there are various repair pathways including mismatch repair, nucleotide excision repair, SSB and DSB repair. The focus here will be on DSB repair due to its known association with viral infections which will be later outlined in further detail.

Homologous recombination (HR) and non-homologous end joining (NHEJ) are the two major repair pathways that can be activated after the detection of a DSB (**figure 1.3**). The phosphatidylinositol 3-

kinase-related kinases (PIKKs) ATM and ATR are central mediators to HR repair. During HR, ATM autophosphorylates (at serine 1981) and phosphorylates H2AX (γH2AX) as well as components of the MRN complex (Mre11-Rad50-Nbs1) which amplify the DDR to recruit further targets including MDC1, 53BP1 and BRCA1 to repair foci (Derheimer and Kastan, 2010). Single stranded DNA (ssDNA) is then generated and coated in RPA which is an ATR target. ATR associates to sites of damage through various components including ATR interacting protein (ATRIP) and TOPBP1 (Cimprich and Cortez, 2008). ATM and ATR can then phosphorylate CHK2 and CHK1 respectively to activate a cellular response via p53. The extensively studied p53 induces transcription of cellular factors involved in inducing apoptosis (e.g. PUMA and BAX proteins) and cell cycle arrest (e.g. CDK inhibitor p21). ATM regulation occurs through activation of the WIP1 phosphatase of which ATM is a target. HR can only occur during S phase and G2 due to the requirement of the sister chromatid for template mediated repair. However, NHEJ can occur at any stage in the cell cycle. NHEJ is mediated by a third major PIKK, DNA dependent protein kinase (DNA-PK) (Burma and Chen, 2004). DSBs are recognised by DNA-PK catalytic subunit, DNA-PKcs, Ku70 and Ku86, collectively known as the Ku complex, before joining of DNA ends by the recruited DNA ligase IV-XRCC4 complex.

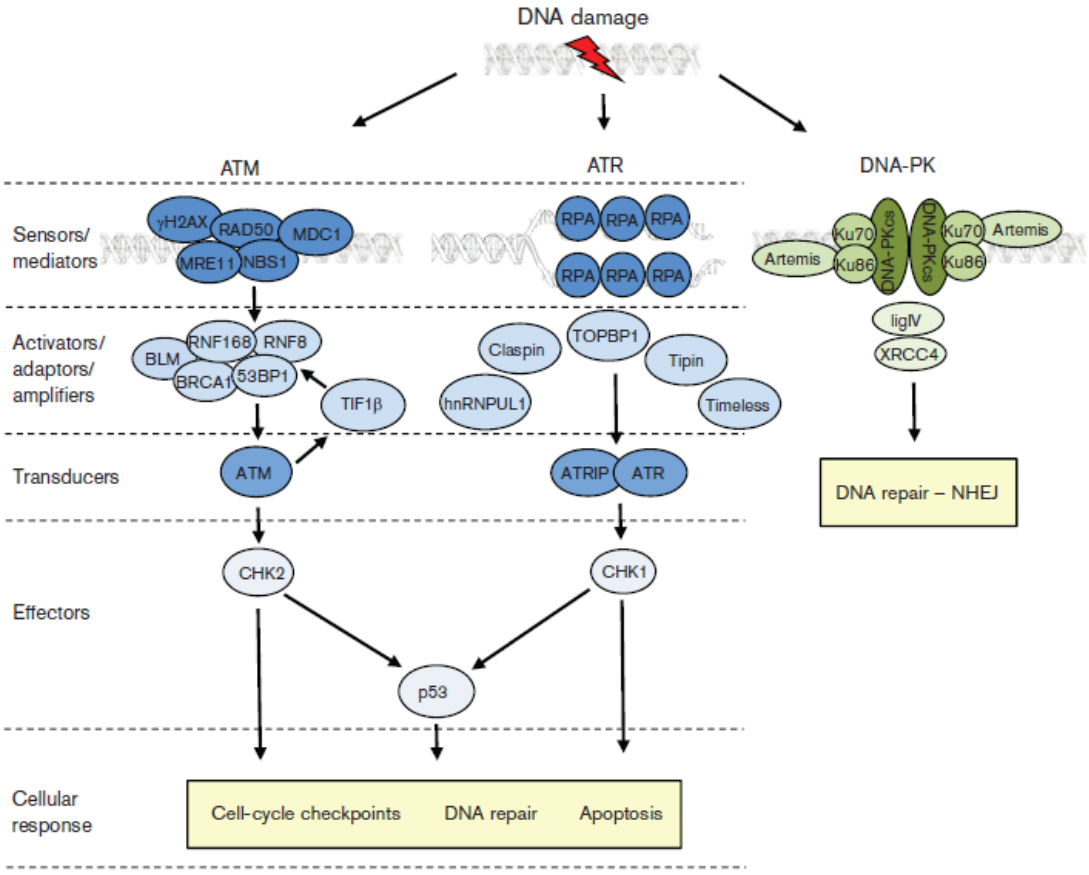


**Figure 1.3 ATM, ATR and DNA-PK signalling pathways in response to DNA double strand breaks.** During homologous recombination, the MRN complex together with phosphorylated H2AX and MDC1 detect DNA damage lesions. The signal is amplified by BRCA1, 53BP1 and others shown allowing downstream ATM signalling. RPA binds single stranded DNA and recruits ATR for its activation by multiple proteins notably TOPBP1. ATM/ATR signalling leads CHK2/CHK1 phosphorylation to induce a response cell cycle arrest, DNA repair or apoptosis. DNA can also be repaired by non-homologous end joining mechanisms mediated by the Ku complex recruiting DNA ligase IV and XRCC4. (Adapted from Turnell and Grand, 2012)

## 1.7 The DNA damage response and DNA viruses

DNA viruses appear to have a strong relationship with the DDR. A DDR is observed following most viral infections although in some cases the advantage to the virus is unclear. It has not been fully determined whether the activation of the DDR upon viral infection is due to direct action by the virus or merely a consequence of infection. Is the DDR advantageous to the life cycle of the virus or an unwanted and inhibitory result of its presence? These are key research questions that are currently trying to be answered. As mentioned above, the DDR is a mechanism in place to preserve DNA sequences so they can be passed on to the next generation and logic dictates that DNA viruses would want to do the same. There is evidence in the literature that supports both arguments.

For example, there is DDR activation upon initial adenovirus infection with detectable phosphorylation of H2AX and RPA32. Later on in infection there appears to be an attenuation of DSB repair pathways which occurs by the inactivation of the members of the MRN complex, BLM and DNA ligase IV (Stracker et al, 2002). However, these DDR targets do not appear to be completely consistent across all serotypes. Adenovirus early region 1A (AdE1A) protein up-regulates the expression of p53 as an early event. However, AdE1B55K and AdE4orf6 recruit an E3 ligase to polyubiquitinate p53 for 26S proteasome mediated degradation. This is thought to occur in order to prevent apoptosis of the host cell curing adenovirus infection (Blackford and Grand, 2009). Polyomaviruses have shown a more dependent relationship towards the cellular DDR. Polyomavirus large T antigen shares a functional homology with AdE1A for example in its role in the activation of p53. During infection, virus production has been shown to be significantly decreased in ATM negative cells and in the presence of an ATM inhibitor (Dahl et al, 2005). Mre11 also co-localises with large T antigen at viral replication compartments during the infection of mouse embryonic fibroblasts (Erickson et al, 2012). Papillomavirus infection induces a DDR characterised by an increase in phosphorylated ATM with time and genome amplification has also been

shown to be dependent on ATM as its inhibition prevents the formation of replication foci (Moody and Lamins, 2009). Herpes Simplex Virus (HSV) has a complex and well-studied relationship with the DDR. Infection of fibroblasts leads to increased phosphorylation of ATM, CHK2 and p53. Mre11 and Nbs1 have been shown to be recruited to sites of viral replication but other reports show a decrease in Mre11 expression following infection (Shirata et al, 2005).

### 1.8 EBV and the DNA damage response

EBV has a complex relationship with the DDR depending on the context. It has been suggested that the virus is capable of inhibiting the DDR to enhance its replication. It has been shown that inhibition of ATM favours the transformation of primary B cells into lymphoblastoid cell lines. Within these cells, there is a correlation between DDR activation and EBV-induced hyperproliferation which is attenuated by EBNA-3C (Nikitin et al, 2010). During lytic cycle, EBV can induce the degradation of p53 via a BZLF1 associated E3 ubiquitin ligase (Sato et al, 2009). The relationship between EBV and the DDR is not one directional, there is also clear evidence for a requirement during the life cycle of the virus. The latent protein EBNA1 directly induces the release of ROS and therefore facilitates the generation of damage lesions and induces a DDR. However, complete DDR signalling is prevented by inhibition of ATM through the action of LMP1 (Chen et al, 2008). Thus, it is probable that EBV requires the upstream DDR components such as the damage sensors and mediators rather downstream signal transducers and effectors. There is evidence to support this selective activation but the relationship is not fully characterised.

It has been suggested that BZLF1 promoter activation requires ATM activity, although this is not universally acknowledged (Kudoh et al, 2005; Li et al, 2011). Subsequent to this work, it has been shown that BGLF4 activation leads to ATM-mediated DDR via the phosphorylation of histone acetylase TIP60 (Li

et al, 2011) as outlined in **figure 1.4**. Recruitment of HR proteins such as Rad51 and H2AX to newly synthesised viral DNA has also been reported (Kudoh et al, 2009).

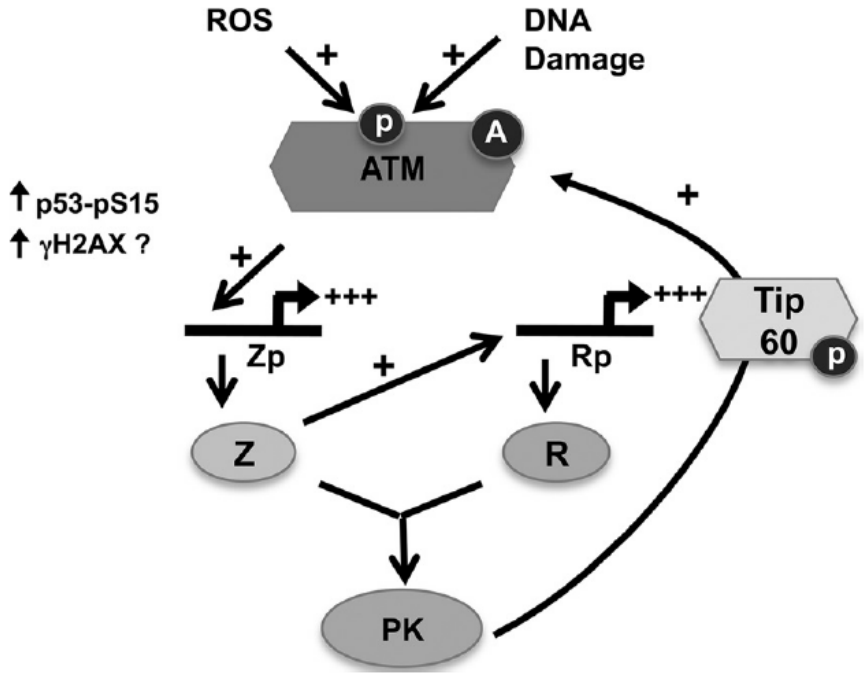


**Figure 1.4 ATM's contribution to theEBV lytic cycle.** ATM is activated by the action of ROS, DSBs and acetylation by TIP60. pATM (ser1981) then contributes to the activation of the BZLF1 promoter. BZLF1 (Z) induces the other immediate early gene, BRLF1 (R), both of which induce the early gene BGLF4 (PK). BGLF4 is then responsible for the phosphorylation of TIP60 (adapted from Hagemaeier et al, 2012).

## 1.9 Aims

Several different DNA viruses, including EBV have been shown to utilise components of the DNA damage response in order to replicate their genomes efficiently. Induction of the EBV lytic cycle is usually examined in inappropriate cell lines induced into the lytic cycle in a non-physiological manner. However, primary differentiated tonsillar epithelial cells do not require such induction because they are naturally lytic. We therefore aim to determine if EBV requires elements of the DDR in a physiologically appropriate cellular background. Our main aims for this project are as follows: 1) Determine if EBV lytic cycle initiates a DDR during lytic cycle. 2) Determine which components of the DDR are being induced by the EBV lytic cycle. 3) Determine if EBV proteins directly interact with components of the DDR. 4) Determine the role of ATM on the EBV lytic cycle.

# 2. MATERIALS AND METHODS

## 2.1 Cells and tissue culture

HEK293, 2089-293, 293-BGLF4KO and Akata cells were maintained in complete medium (RPMI-1640, 10% foetal calf serum (FCS), 1% glutamine and 1% penicillin/streptomycin). 2089-293 and BGLF4KO-294 are HEK293 cells containing recombinant B95.8 strain EBV bacterial artificial chromosome (BAC) which encodes a hygromycin-resistance and GFP cassette. Akata-GFP is a recombinant Akata strain EBV BAC maintained in EBV-loss Akata BL cells encoding a G418-resistance and GFP expression cassette. The 2089-293 and BGLF4KO-293 medium was supplemented with 100μg/ml Hygromycin (Sigma) and the Akata-GFP medium was supplemented with 50μg/ml G418 cells to maintain the BAC in the cell lines. The BGLF4-293 cells were kindly provided by H.J. Delecluse. Tonsils were obtained from the Human Biomaterials Resource Centre (HBRC), Birmingham, following routine tonsillectomies. Primary epithelial cells derived from tonsils were maintained in Keratinocyte-SFM medium (Life Technologies).

## 2.2 Induction of EBV lytic cycle and transfections

The EBV lytic cycle was induced by transfecting the 2089-293 (BGLF4KO-293) cells with a plasmid encoding the immediate early inducer of viral lytic replication, BZLF1. One microgram of the BZLF1 (pRA) and the gp110 (p509) expression plasmids were incubated with 6μl of Lipofectamine (Life Technologies) in 100μl OptiMEM (Life Technologies) at room temperature for 30 minutes. The transfection mix was topped up to 1ml with OptiMEM and added to $2x10^6$ 2089-293 cells in 1 well of a 6-well plate. The cells were incubated with the transfection mix for 3 hours at 37°C then topped up with 1ml complete medium. The induced 2089-293 cells were harvested at appropriate times following transduction. EBV-

negative 293 cells transfected with BALF2, BMRF1, BMLF1 or BGLF4-HA plasmids (all cloned into pcDNA3 expression vectors) underwent the same method of transfection and harvested at 24 hours. Semi-confluent Akata cells were resuspended at $4x10^6$ cells/mL in RPMI-1640 1% FCS and supplemented with goat anti-human IgG $(Fab')_2$ at 0.5% v:v (50μg/ml). The cells were incubated for 3 hours at 37°C then diluted to $1x10^6$ cells/mL with complete medium. The virus-containing medium was harvested 72 hours post induction and quantified.

### 2.3 Virus purification and infection of primary keratinocytes

Purification of infectious virus particles was carried out in order to enhance entry into primary keratinocytes. A 60% solution of OptiPrep was diluted to give a 30% solution with OptiPrep diluent (0.85% (w/v) NaCl, 60mM Hepes-NaOH, pH 7.4). Two polyallomer ultracentrifuge tubes were made up as follows: One mL of 30% OptiPrep was overlaid with 10ml Akata virus supernatant and ultracentrifuged using a SW40 swing rotor for 2 hours at 20,000RPM, 4°C. This concentrated the virus on an Optiprep cushion. Nine ml of virus supernatant was removed and discarded and the remaining 2ml virus plus Optiprep from both tubes were thoroughly mixed and placed in a 4.8mL ultracentrifuge tube, topped up with 15% Optiprep. The virus was then ultracentrifuged in a vTi60.5 vertical rotor for 2 hours 30 minutes at 64,000RPM, 4°C to generate a density gradient in which the intact virus bands. The single white band of intact virus was removed by needle and syringe. The virus was then diluted 1 in 10 with Keratinocyte SFM.

Primary keratinocytes were initially incubated with integration-deficient CD21-expressing lentivirus (provided by C. Shannon-Lowe) to facilitate CD21-mediated viral entry. The lentivirus was removed after 24 hours at maximal CD21 expression and replaced with purified Akata virus supernatant for 24 hours.

The GFP-positive epithelial cells were sorted by FACS for GFP expression as a marker of EBV infection. The cells were then harvested for RNA analysis.

## 2.4 Antibodies

Antibodies used to detect EBV proteins by immunofluorescence and Western blot are shown in **table 2.1**. Antibodies to detect DNA damage response proteins are shown in **table 2.2**. All antibodies for immunofluorescence (IF) were diluted in 10% heat inactivated normal goat serum (HINGS) and antibodies used for WB were diluted in 5% w/v dry milk powder in TBS-Tween except where stated otherwise.

| Target | Clone | Species | Application (dilution) | Provider/Reference |
|---|---|---|---|---|
| BZLF1 | BZ.1 | Mouse | IF (1/50), WB (1/1000) | M. Rowe |
| BRLF1 | 11-008 | Mouse | IF (1/500), WB (1/1000) | Argene |
| BHRF1 | 5B11 | Mouse | IF (1/200), WB (1/100) | Chemicon |
| BGLF4 | RB03734 | Rabbit | IF (1/100), WB (1/200), IP | Abgent |
| BMRF1 | R3 | Mouse | IF (1/200), WB (1/2000), IP | Chemicon |
| BMLF1 | EB2 | Rabbit | IF (1/100), WB (1/5000), IP | Buisson et al, 1999 |
| BALF2 | OT13-B | Mouse | IF (1/2000), WB (1/4000), IP | J. Middeldorp |
| BALF5 | - | Rat | IF (1/100), WB (1/1000) | F. Grasser |

**Table 2.1. Antibodies used in this study to examine EBV lytic gene expression**. All antibodies are shown at the dilutions used for either Western blot or immunofluorescence.

| Target | Clone | Species | Application (Dilution) | Provider/Reference |
|---|---|---|---|---|
| ATM | D2E2 | Rabbit | WB (1/1000)* | Cell Signalling |
| ATM | AB82512 | Rabbit | IF(1/200) | Abcam |
| pATM (Ser1981) | AB81292 | Rabbit | IF (1/200) | Abcam |
| pATM (Ser1981) | 10H11.E12 | Mouse | WB (1/1000)* | Cell Signalling |
| ATR | E1S3S | Rabbit | WB (1/1000) | Cell Signalling |
| pATR (Ser428) | 2853 | Rabbit | WB (1/1000)* | Cell Signalling |
| p53 | D01 | Mouse | WB (1/200) | R. Grand |
| Mre11 | 4895 | Rabbit | WB (1/1000) | Cell Signalling |
| H2AX | D17A3 | Rabbit | IF (1/1000), WB (1/1000) | Cell Signalling |
| γH2AX (Ser139) | JBW301 | Mouse | WB (1/1000) | Millipore |
| γH2AX (Ser139) | AB11174 | Rabbit | WB (1/1000) | Abcam |
| Rad50 | AB3623 | Rabbit | IF (1/100), WB (1/1000) | Abcam |
| Rad51 | H-92 | Rabbit | IF (1/50), WB (1/1000) | Cell Signalling |
| RPA32 | AB-2 | Mouse | WB (1/1000) | Calbiochem |
| RPA32 | A300-244A | Rabbit | WB (1/1000) | Bethyl |
| pRPA (Ser4/Ser8) | A300-245A | Rabbit | IF (1/1000), WB (1/1000)* | Bethyl |
| NBS1 | AB7860 | Mouse | WB (1/1000), IF (1/100) | Abcam |
| pNBS1 (Ser278) | AB111373 | Rabbit | WB (1/1000) | Abcam |
| CHK2 | - | Rabbit | WB (1/1000) | G. Stewart |

**Table 2.2. Antibodies used in this study to examine DNA damage response proteins**. All antibodies are shown at the dilutions used for either Western blot of immunofluorescence. *5% w/v BSA in TBS-Tween.

| Target | Clone | Species | Application (Dilution) | Provider/Reference |
|---|---|---|---|---|
| Actin | AC-40 | Mouse | WB (1/4000) | Sigma |
| Calregulin | C4606 | Rabbit | WB (1/2000) | Sigma |
| HA | - | Mouse | WB(1/1000), IP | R. Grand |

**Table 2.3. Antibodies used in control experiments**. All antibodies are shown at the dilutions used for either Western blot of immunofluorescence.

| Target | Species | Application (dilution) | Provider/Reference |
|---|---|---|---|
| Rat IgG (Alexa-Fluor-488) | Goat | IF (1/1000) | Life Technologies |
| Mouse IgG (Alexa-Fluor-488) | Goat | IF (1/1000) | Life Technologies |
| Mouse IgG (Alexa-Fluor-594) | Goat | IF (1/1000) | Life Technologies |
| Rabbit IgG (Alexa-Fluor-488) | Goat | IF (1/1000) | Life Technologies |
| Rabbit IgG (Alexa-Fluor-594) | Goat | IF (1/1000) | Life Technologies |
| Mouse IgG (HRP conjugated) | Goat | WB(1/1000) | Sigma |
| Rabbit IgG (HRP conjugated) | Goat | WB (1/2000) | Sigma |
| Rat IgG (HRP conjugated) | Goat | WB (1/1000) | Sigma |

**Table 2.4. List of secondary antibodies**. All antibodies are shown at the dilutions used for either Western blot of immunofluorescence.

## 2.5 Western blotting

Cells were removed of growth medium and washed with sterile PBS before harvesting and dilution in 9M urea. These samples were then lysed by sonication and the concentration was determined by absorbance readings relative to 1ug/ul BSA. 20ug of sample was loaded (with equal volume gel sample buffer (9M urea, 50mM Tris HCl pH 7.4, 10% SDS, 0.15M β-mercaptoethanol, 0.1% bromophenol blue) onto an acrylamide gel. Gels were then wet transferred onto nitrocellulose membrane in transfer buffer (0.05M Tris, 0.19M glycine, 20% methanol) at 280mA for 6 hours. Membranes were blocked for 1 hour with 5% w/v dry milk or 5% w/v BSA in TBS-Tween before incubation with primary antibodies overnight at 4°C. Following washing, secondary antibodies (HRP linked) were incubated with the membranes for 2 hours at room temperature. A final TBS-Tween washing stage precede the addition of ECL reagent for 1 minute followed by detection of bands via X-ray film.

## 2.6 Co-immunoprecipitation (Co-IP)

For each IP experiment (including controls), $2x10^7$ cells were harvested, pelleted and kept on ice. The pellet was resuspended in 1mL NETN buffer (1% NP40, 0.15M NaCl, 5mM EDTA, 50mM Tris, pH to 7.4) and lysed with a Wheaton-Dounce homogeniser. The following centrifugation steps then took place saving the supernatant at each step: 5 minutes at 3000RPM, 5 minutes at 13000RPM, 30 minutes at 45000RPM. The supernatant was then incubated with 5ug of antibody overnight at 4°C followed for a further centrifugation at 45000RPM. The samples were then incubated for 2 hours with 50ul of Protein G beads per 1mL of supernatant and spun for 2 minutes at 3000RPM, discarding the supernatant and then washing the pellet with NETN buffer. The final pellets were resuspended in 50ul gel sample buffer, boiled at 85°C for 3 minutes and loaded on to a 10% acrylamide gel for Western blot analysis.

## 2.7 Mass Spectrometry

Cells were harvested and treated in the same manner as co-immunoprecipitation samples with the exception of the final resuspension in gel sample buffer and Western blot analysis. The pellets were instead washed twice with detergent-free NETN buffer and then denatured in 9M Urea/50mM ammonium bicarbonate (ABC) for 30 minutes at room temperature. After centrifugation, protein was collected from the supernatant and reduced with 50mM dithiothreitol (DTT) in 50mM ABC for 30 minutes at 56°C and alkyated with 100mM iodoacetamide (IAA) for 30 minutes at room temperature in the dark. The protein was recovered using Amicon centrifugal filters (30K cut off) which were washed four times with 50mM ABC. Protein was then digested with 1ug of sequencing grade trypsin overnight at 37°C added to the washed filters. The peptides were retrieved by centrifugation of the filters which were washed with 300µL of ABC. Combined supernatants containg the tryptic peptides were dried in a vacuum centrifuge, resuspended in 1% acetonitrile/1% formic acid and loaded onto the mass spectrometer.

## 2.8 RNA extraction, DNase digestion and cDNA synthesis

RNA was extracted from the cells using the Nucleospin II kit (Macherey-Nagel) according to manufacturer's instructions. The RNA was subjected to a further DNAse treatment to remove all remaining DNA using the DNAfree kit (Ambion, Life Technologies). One microgram of RNA was incubated with 1µl DNase at 37°C for 30 minutes then inactivated with the inactivation solution for 2 minutes. The RNA samples were centrifuged to remove the inactivation solution and 10µl (400ng) was removed for the cDNA synthesis. The treated RNA was added to 4µl Q-Script (VWR) and incubated at 42°C for 1 hour followed by inactivation at 95°C for 5 minutes to give a final concentration of 5ng/µl of cDNA.

A recombinant plasmid containing 45 EBV amplicons and 3 cellular amplicons (known as the absolute quantification (AQ) plasmid) (see appendix I) was cloned into a pUC57 vector (GenScript) and used to generate a standard curve for qPCR. FAM/TAMRA labelled Taqman real-time PCR assays were designed for each individual EBV gene. The three control assays included Glyceraldehyde 3-phosphate dehydrogenase (GAPDH), Beta-2-microglobulin (B2M) and Phosphoglycerate kinase 1 (PGK1) (Life Technologies). 25ng of test sample DNA and 10 fold dilutions of the quantification plasmid were used to amplify the target genes. Specific target amplification was carried out on 25ng of DNA using 1.25µL primer mix (45 EBV and 3 cellular) and PreAmp Master Mix (Life Technologies) in DNA suspension buffer (10mM Tris, pH 8.0, 0.1mM EDTA) as instructed. After 95°C heating for 10 minutes, samples underwent 12 cycles of 95°C for 15 seconds followed by 60°C for 4 minutes. 1 in 5 dilutions were prepared and loaded on to 48:48 Dynamic Array IFC (Fluidigm), run in a Biomark HD machine and analysed using Biomark Real-Time PCR Analysis Software Version 2.0.

### 2.9 Immunofluorescence microscopy

Following EBV infection or lytic cycle induction, cells were trypsinised and incubated overnight at 37°C on fibronectin coated 8-well chamber slides ($2x10^4$ cells per well). The cells were fixed with 4% paraformaldehyde (PFA) for 20 minutes at RT, permeabilised with 0.5% Triton X-100 for 5 minutes at RT then blocked in 10% HINGS for 1 hour at RT. The cells were then incubated with diluted primary antibodies for 1 hour at 37°C, thoroughly washed in PBS then incubated with the appropriate secondary antibodies. Slides were then mounted in DAPI-containing Vectashield mounting buffer (Vector labs). The cells were analysed using a Carl Zeiss 510 Confocal microscope and LSM 5 image browser.

## 2.10 Induction of DNA damage and inhibitor treatments

To induce DNA damage for positive controls, confluent cells were treated with ionizing γ-rays from a $^{137}Cs$ source at a dose of 6Gy radiation. After 1 hour at 37°C, cells were fixed with 4% PFA for immunofluorescence microscopy as above or harvested for either western blot or RT-qPCR analysis.

For ATM inhibitor treatment experiments, cells were treated with either 0μM (DMSO only), 1μM, 5μM or 10μM of the inhibitor KU55933 (Calbiochem) for 1 hour. Cells were harvested for analysis by RT-qPCR, western blot or counted to quantify cell viability which was determined by uptake of Trypan Blue. Adherent cells and cells detached in medium were counted.

# 3. RESULTS

## 3.1 EBV lytic protein expression and the ATM/ATR response

We initially wanted to determine when the EBV genes of interest were expressed following induction into lytic cycle. 2089 cells were induced into lytic cycle by transfection with BZLF1 and harvested at 0, 12, 24, 48 and 72 hours post induction and subjected to Western blotting (**figure 3.1**). The gp110 expression vector (pRA) was co-transfected with the BZLF1 expression vector (p509) in order to produce complete and infectious virus particles as the 2089 sequence contains a small deletion in the gp110 gene. Expression of the immediate early and early proteins analysed, began between 12 and 24 hours post induction and then increased throughout the entire time course. The 0 hour time point represents a no plasmid transfection. The transfected BZLF1 is expressed at 24 hours and stimulates the expression of the other immediate early gene, BRLF1. These stimulate the expression of the early lytic genes which are involved in the replication of viral DNA. All proteins are significantly expressed by 48 hours. There is no distinct difference in expression patterns between the proteins analysed.

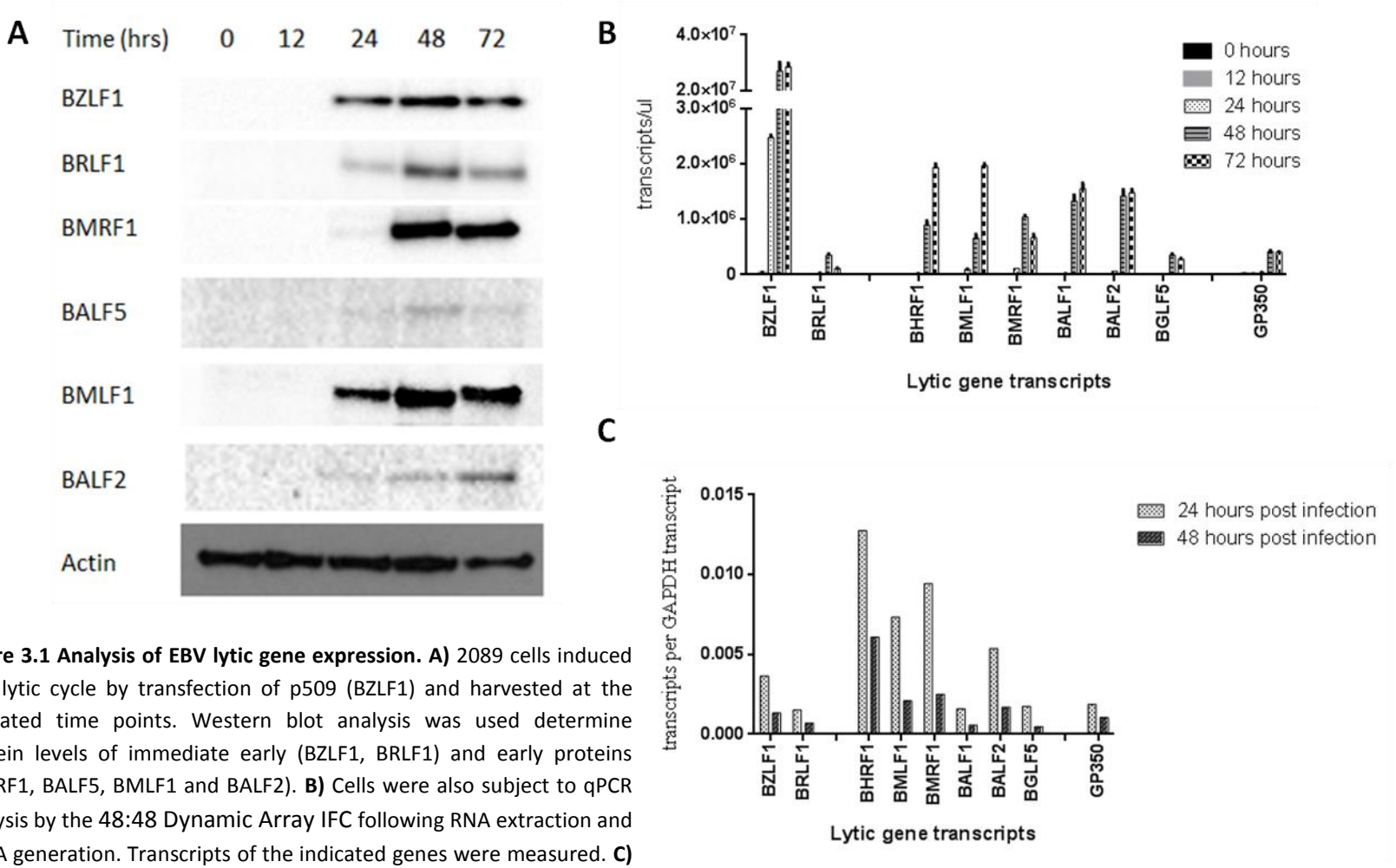


**Figure 3.1 Analysis of EBV lytic gene expression. A)** 2089 cells induced into lytic cycle by transfection of p509 (BZLF1) and harvested at the indicated time points. Western blot analysis was used determine protein levels of immediate early (BZLF1, BRLF1) and early proteins (BMRF1, BALF5, BMLF1 and BALF2). **B)** Cells were also subject to qPCR analysis by the 48:48 Dynamic Array IFC following RNA extraction and cDNA generation. Transcripts of the indicated genes were measured. **C)** Primary keratinocytes were infected with CD21-expressing lentivirus for 24 hours followed by infection with Akata-GFP virus and sorted based on GFP positivity. Cells were harvested and RNA extracted before for being subject to the same qPCR analysis as 2089 cells in **B.**

To compare the dynamics of EBV lytic replication in a more physiologically relevant model, primary keratinocytes were obtained for analysis following routine tonsillectomies. Once in culture, cells began to differentiate, making it possible for EBV to undergo lytic cycle once the virus has entered. To facilitate entry of the virus, cells were infected with CD21-expressing lentivirus as this protein is known to be essential for B cell infection (Nemerow et al, 1987). After a 24 hour incubation period, cells were then washed and infected with recombinant Akata (GFP-positive) strain EBV for 24 hours and sorted for GFP positivity to purify the cells of interest. Cells were then harvested immediately or cultured a further 24 hours (48 hours post EBV infection) and then harvested. RNA was extracted from cells and cDNA generated for qPCR analysis using a 48:48 Dynamic Array IFC as described in materials and methods. Gene expression is shown for the major lytic genes BZLF1, BRLF1, BHRF1, BMLF1, BALF1, BALF2, BGLF5 and GP350 (**figure 3.1C**). 2089 cells harvested at 0, 12, 24, 48 and 72 hours were subjected to the same qPCR analysis (**figure 3.1B**).

Gene expression was relatively low compared to the 2089 model and the data were normalised to GAPDH transcripts. No obvious host cell protein synthesis shut off was observed. Expression appears to be higher at 24 hours rather than at later time points as previously seen in our cell line. A 2-fold decrease is apparent in all gene transcript levels at 48 hours. This is also true for each subset of the lytic genes: immediate early, early and late. Due to the low number of cells available for this experiment, it was not possible to carry this out in duplicate and a 72 hour time point could not be investigated. Due to circumstances out of our control, no further experiments could be carried in these cell types.

In order to determine the time after lytic induction that the viral proteins involved in viral DNA replication may affect the DNA damage response, we performed a time course experiement for 72 hours. The harvested cells were subjected to Western blot analysis for H2AX, Nbs1, ATM, CHK2, RPA,

ATR and their phosphorylation at damage associated sites examined. 2089 cells were transfected with BZLF1 and with or without gp110. Cells subjected to transfection of gp110 only acted as a negative control for DDR activation. No lytic gene expression was observed with the transfection of gp110, therefore any response in this subset is attributable to the cells responding to the presence of foreign DNA.

ATM and its selected down-stream targets H2AX, RPA and CHK2 (including their phosphorylated forms) were identified as seen in **figure 3.2**. Over time, the phosphorylation of H2AX (seen as γH2AX) increases significantly, from virtually no detectable protein at 0 hours, indicating a damage response has been activated. There may be a slight upregulation in ATM expression over time but not greatly. ATR and its downstream target, RPA, were also detected as well as DNA damage associated phosphorylation. A slight increase in RPA expression is detectable at 48 and 72 hours post transfection where we see expression of immediate early and early EBV lytic genes as shown in **figure 3.1A and B**. In the mock transfected cells, the total (and phosphorylated) protein expression trends are mirrored in each case for both ATM, ATR and their downstream targets. These trends cannot therefore be solely attributed to action of viral proteins. A notable result is the phosphorylation of Nbs1, at 12 and 24 hours post induction, in the mock transfected cells which is not visible in the lytic cells.

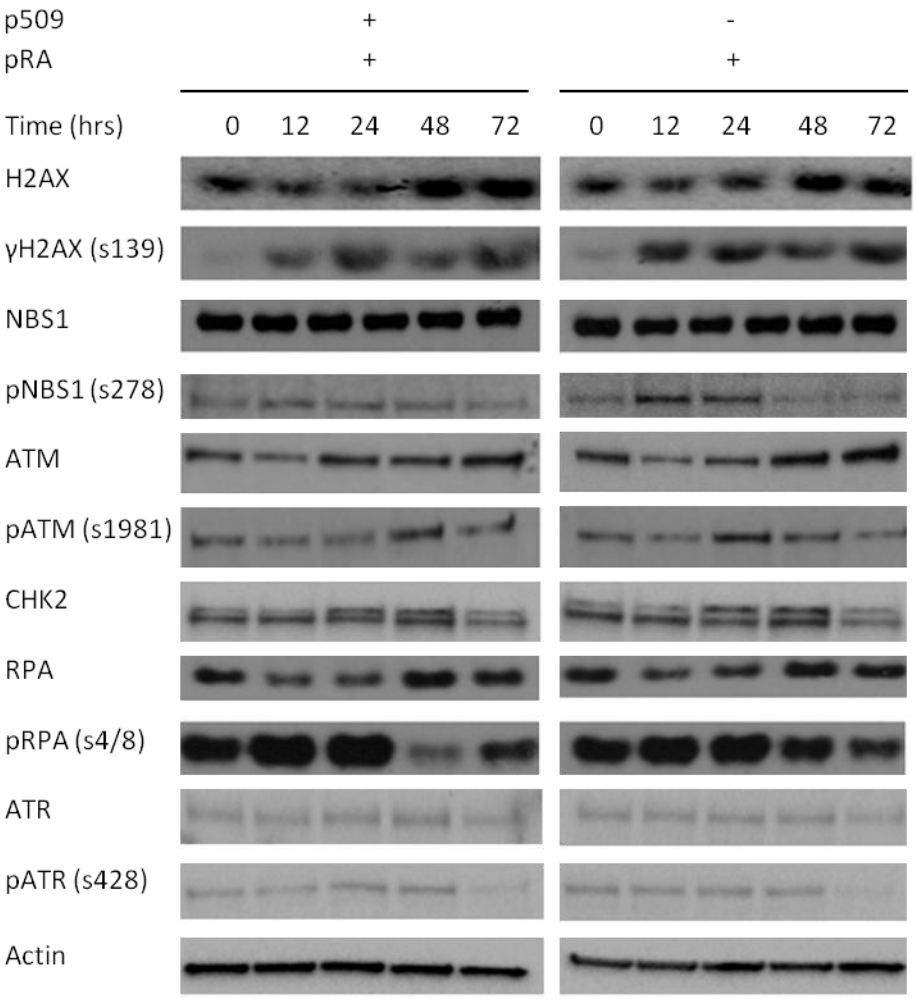


**Figure 3.2 Analysis of the DNA damage response during lytic replication.** 2089 cells induced into lytic cycle by transfection of p509 (BZLF1) and pRA (gp110) and harvested at the indicated time points. Western blot analysis was used determine protein levels of ATM, ATR and their respective targets as indicated.

### 3.2 Co-localisation of EBV lytic proteins and components of the DNA damage response

Given that induction into lytic cycle did appear to alter expression or phosphorylation of DDR proteins relative to our controls, we decided to investigate the localisation of both viral cellular DDR proteins in lytic cells. A representative panel of DDR proteins was investigated by immunofluorescence microscopy during EBV lytic cycle. Initially, the proposed antibodies to be used for these experiments were tested for their ability to detect damage foci and were optimised using 293 cells. 293 cells grown on chamber slides were treated with 6Gy of gamma-radiation or left untreated, fixed after 1 hour and stained as appropriate **(figure 3.3)**. The irradiated cells clearly show the formation of damage foci, due to the induction of DSBs, by the recruitment of γH2AX, pATM and NBS1 to specific compartments within the nucleus relative to the untreated cells. There is less obvious formation of foci with pRPA, Rad50 and Rad51 but a clear difference in staining pattern when compared to unirradiated cells. Other candidates were also tested (data not shown) but showed no difference between untreated and irradiated cells and were therefore not taken further.

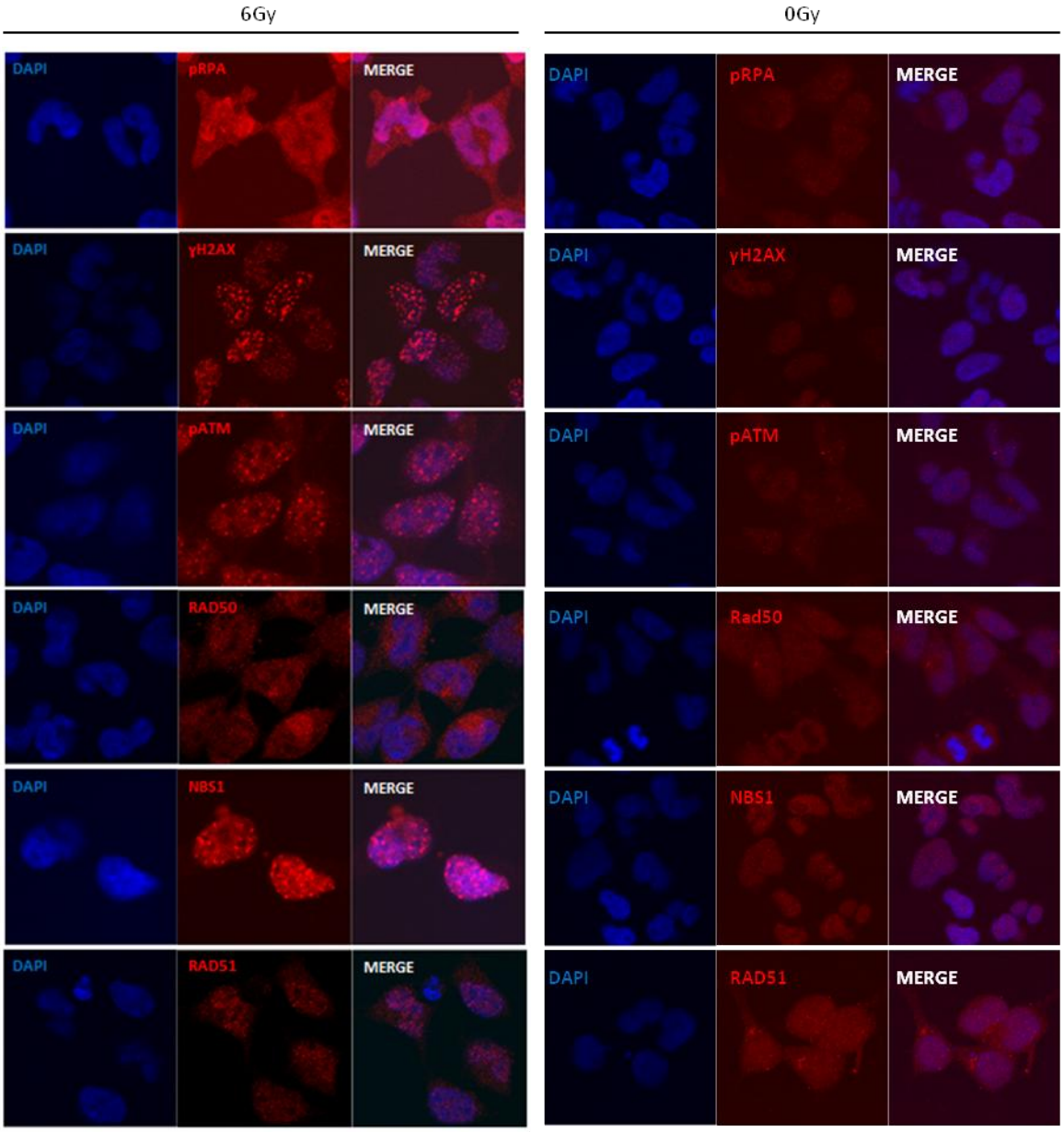


**Figure 3.3 Optimisation of antibody concentrations.** 293 cells were treated with either 6Gy radiation or left untreated and fixed after 1 hour. At varying concentrations, slides were then stained for DNA damage foci associated proteins pRPA, γH2AX, pATM, Rad50, Nbs1 and Rad51. Concentrations detecting damage foci shown.

In order to investigate the co-localisation between EBV lytic proteins and DNA damage components, 2089 cells were induced into lytic cycle as previously described and plated on to chamber slides for immunofluorescence staining and fixed at 24 hours post induction. Cells were then either stained for the viral DNA binding protein, BALF2, or the viral polymerase accessory protein, BMRF1, with various anti-DDR antibodies. These viral proteins were chosen for their central role in viral DNA replication. Representative immunofluorescence experiments are shown (**figures 3.4 and 3.5**). Each figure shows the localisation of pRPA, Rad51, pATM and Rad50 in lytic 2089 cells. For each pairing of proteins, the immunofluorescent image has been shown with a merge to visually analyse co-localisation by the presence of pixels expressing yellow, a false colour representing co-localised proteins. Viral replication compartments are known to occur in the nucleus, therefore the pixels representing the nucleus have been analysed as our region of interest (ROI) for the scatter graphs shown. The scatter graphs allow the isolation of pixels expressing intensity of ≥50% of maximal intensity (regions 1, 2 and 3) for analysis. This was done to differentiate between background and real and specific protein staining. Region 3 pixels represent co-localisation. Co-localisation coefficients are calculated based on co-localised pixels as a proportion (minimum: 0, maximum: 1) of total intense pixels for each colour (i.e. protein). Region 1 and region 2 represent highly intense pixels, detecting viral and cellular proteins respectively, that have not co-localised.

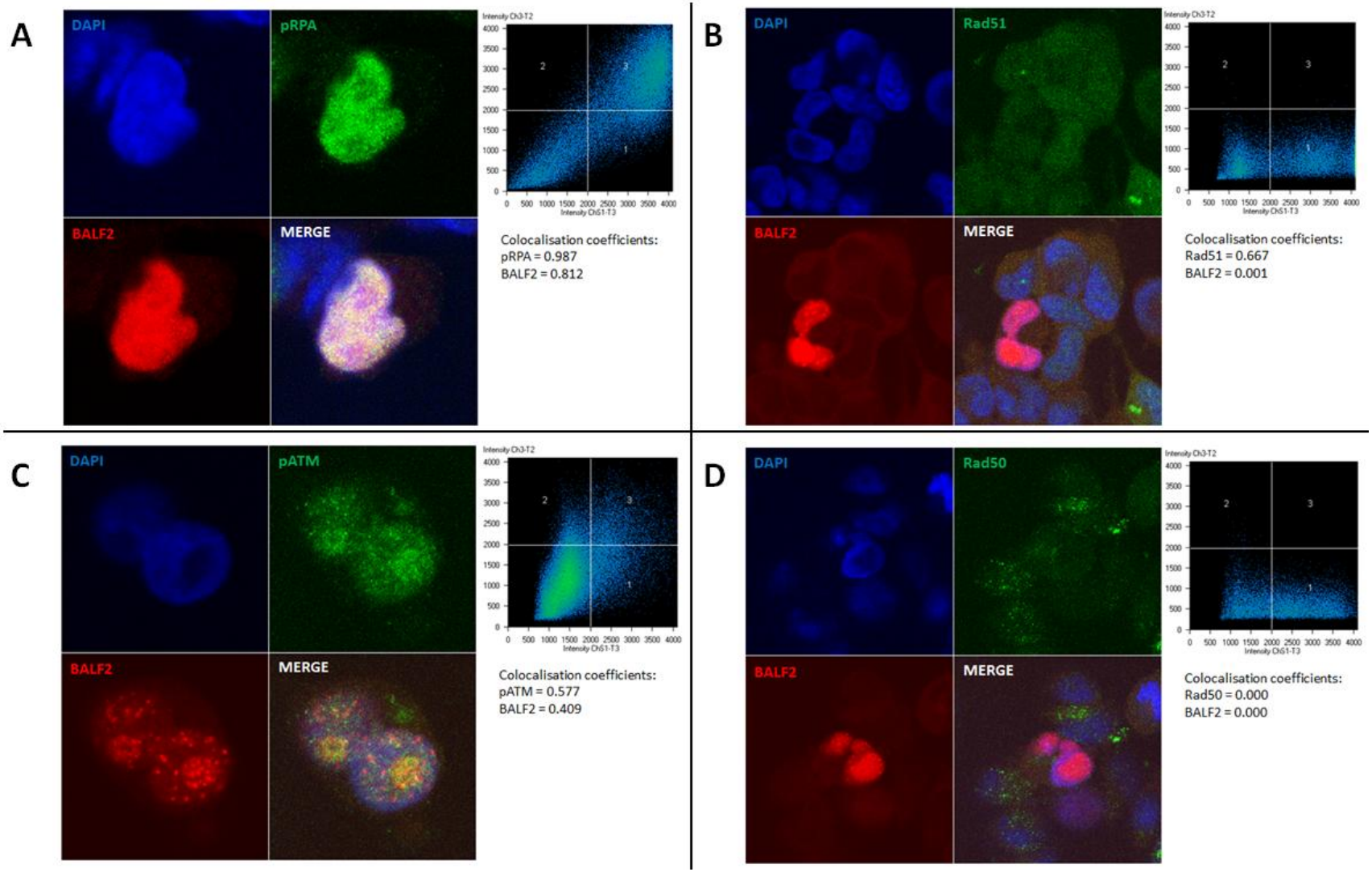


**Figure 3.4 Co-localisation of BALF2 with DNA damage proteins.** 2089 cells were induced into lytic replication and fixed onto slides at 24 hours post induction. Cells were then stained for BALF2 (red) and either **A)** pRPA **B)** Rad51 **C)** pATM or **D)** Rad50. Co-localisation coefficients were then calculated based on the pixels of high intensity within the region of interest (nuclei of lytic cells).

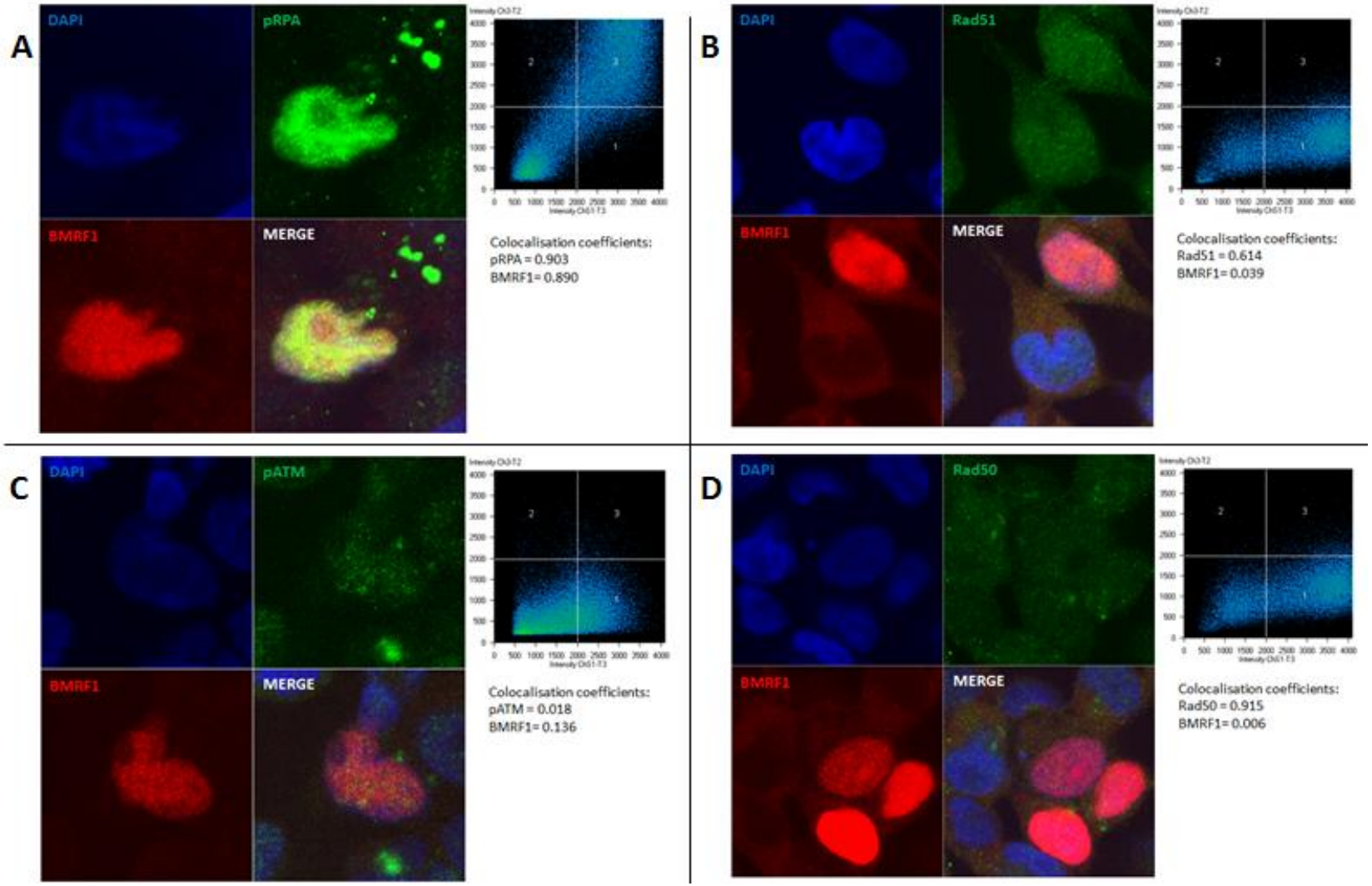


**Figure 3.5 Co-localisation of BMRF1 with DNA damage proteins.** 2089 cells were induced into lytic replication and fixed onto slides at 24 hours post induction. Cells were then stained for BMRF1 (red) and either **A)** pRPA **B)** Rad51 **C)** pATM or **D)** Rad50. Co-localisation coefficients were then calculated based on the pixels of high intensity within the region of interest (nuclei of lytic cells).

There is a strong association between pRPA and BALF2 localisation (**figure 3.4A**). The staining shows a high level of co-localisation between the two proteins but in the absence of distinct foci or replication compartments. The images selected are representative of the staining pattern throughout but there was some variation in the presence or absence of distinct foci between cells. Analysis of the scatter graphs here shows that a significant proportion of the highly intense pixels have co-localised. The coefficients determined that 98.7% of the pixels showing staining for pRPA are also staining for BALF2 (and vice versa for the BALF2 pixels at 81.2%). Such intense staining for pRPA was not seen in non-lytic lytic cells. A similar relationship is evident between BALF2 with pATM (**figure 3.4C**) but to a lesser extent. Here, proportionally, there are many more pixels staining at a high intensity that are independent from each other compared to the relationship seen for BALF2 and pRPA. **Figures 3.4B and 3.4D** show the lack of co-localisation of BALF2 with Rad51 and Rad50 respectively. Very few pixels, if any, are staining with a high enough intensity to suggest real staining rather than background. In each case BALF2 is only showing a co-localisation coefficient of 0.001 for Rad51 and 0.000 for Rad50.

BMRF1 was co-stained with the same cellular proteins for comparison and similar results are seen in certain circumstances. A high intensity of staining is present in the nuclei of lytic cells for pRPA (**figure 3.5A**) and again shows a close association with the viral protein. A different pattern of pATM staining (**figure 3.5C**) is observed when co-stained with BMRF1. The images suggest very little co-localisation is occurring, which is confirmed by the low coefficient values. The distribution of pATM does not seem to differ between the lytic cells and surrounding cells that have not entered lytic cycle. **Figures 3.5B and 3.5D** show staining for Rad51 and Rad50 with BMRF1, respectively. Similar patterns are seen here as with BALF2, however these DDR proteins have not stained strongly enough in this case to confidently identify specific staining from background. Little association is visible within the images and these

correspond to the low coefficient values. BMRF1 appears to be present in the cell independently of both Rad51 and Rad50.

### 3.3 Interactions between viral and cellular DDR proteins

In order to determine if the co-localisation of the viral proteins with the DDR proteins, RPA in particular, corresponds to a physical interaction, we performed co-immunoprecipitation (co-IP) experiments. Again, 2089 cells were induced into lytic cycle with BZLF1 and harvested at 24 hours and subject to co-IP. Cell lysates were incubated with antibodies against BMRF1, BALF2 (**fig 3.6A**) and BMLF1 (**fig 3.6B**). Immunoprecipitated proteins were retained on Protein G beads before Western blot analysis. γH2AX was also blotted for due to its previously reported association with EBV lytic cycle (Kudoh et al, 2009). No-antibody samples were included as negative controls and 10μg of 293 lysate was loaded as a positive control for the DNA damage proteins. The presence of a band in the negative control lane for RPA in **figure 3.6A** makes the analysis more difficult, but there seems to be no difference between the control samples and the test samples for BMRF1 and BALF2. This is also true for γH2AX. **Figure 3.6B** shows the presence of a faint band at a long exposure for RPA in the BMLF1 sample which is not present in the negative control.

Co-IP studies were also carried out in order to determine whether viral proteins could interact with RPA and γH2AX independently of the lytic cycle. This was done in order to determine if any interactions observed from the 2089 cells were dependent on other viral proteins. 293 cells were transfected (or left untransfected for negative controls) with plasmids containing either BMRF1 (**figure 3.6C**), BALF2 (**figure 3.D**), BMLF1 (**figure 3.6E**) or BGLF4 (HA tag) (**figure 3.6F**). After 24 hours the cells were harvested, lysed, incubated with appropriate antibody and analysed by Western blot for RPA and γH2AX binding. An anti-

HA antibody was used to immunoprecipitate BGLF4. Again, 10µg of 293 cell lysate was used as a positive control for the DDR antibodies. As a negative control, the same viral antibody was used but with the lysate of untransfected 293 cells (panel **C to F**). In each case, no obvious difference was observed between negative control and test samples. This is significant for BMLF1 and RPA which in previous analysis have given a positive result (**figure 3.6B**).

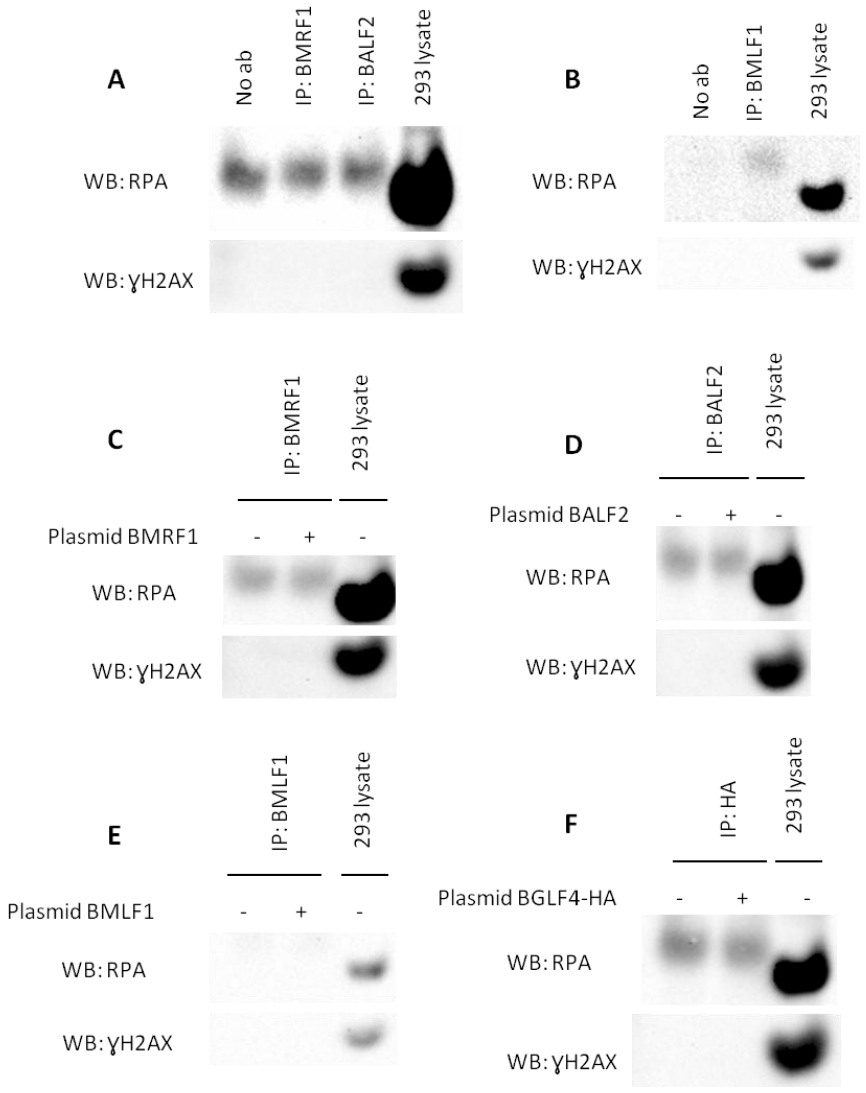


**Figure 3.6 Interactions between RPA and γH2AX with viral lytic proteins. A and B:** 2089 cells induced into lytic cycle by transfection of p509 (BZLF1) and harvested at 24 hours. Antibodies against BMRF1, BALF2 and BMLF1 were used to IP followed by Western blot analysis. **C to F:** 293 cells transfected with plasmids for BMLF1, BMRF1, BGLF4 (HA), BALF2 or transfected and harvested at 24 hours. The appropriate antibody was used to IP, alongside untransfected 293 controls, followed by Western blot analysis. 293 lysate was used as a positive control.

To identify further potential interactions for viral proteins with DDR proteins and other cellular components, mass spectrometry analysis of induced 2089 cells followed. As previously described, 2089 cells were induced into lytic cycle and harvested at 24 hours. Lysates were then immunoprecipitated with BMRF1, BALF2, BMLF1 or BGLF4. Analysis of samples immunopreciptated by BMRF1, BMLF1 and BGLF4 antibodies all failed to detect any viral proteins. However, BALF2 fragments were detected in the appropriate sample. After excluding proteins also detected in the no-antibody negative control, no known DDR related proteins were observed. The most notable result was an overwhelming 14 identified peptides specific to the LETM1 protein. Although LETM1, a mitochondrial $H^{+}$-$Ca^{2+}$ exchanger, is not a known DDR protein and the result would need to be verified, this is a novel interaction. For comparison purposes, 11 peptides of BALF2 were identified in the sample.

### 3.4 The effects of ATM inhibition on EBV gene expression

ATM is central to the DNA damage response signalling pathways. It has been suggested that it and other aspects of the DDR are required for efficient replication of EBV; it is possible, therefore, that ATM inhibition will have a negative impact. Initially, the ATM inhibitor (ATMi) KU55933 was tested for function at various concentrations suggested in previous reports. 293 cells were treated with 10µL of either DMSO alone, 1µM, 5µM or 10µM (final concentration) of ATMi followed by irradiation and harvesting for Western blot analysis (**figure 3.7A**). As a control, pATM (s1981) and its downstream targets pKAP1, and γH2AX were probed to test the level of phosphorylation, ensuring the ATMi was working. 293 cells, untreated with ATMi or radiation, were used as a control for a non-activated damage response. Most strikingly, the KAP1 phosphorylation decreases to unirradiated levels in the presence of 5µM ATMi. H2AX and ATM phosphorylation remained a little higher than the unirradiated cells at both 5µM and 10µM but there is still an evident reduction.

The toxicity of the ATMi or DMSO treatment was a potential issue which could give misleading results. Cells were treated with concentrations of ATMi as above and counted at time points subsequent experiments. Cells were counted in the presence of Trypan Blue to determine cell viability. Dead cells, which take up Trypan Blue, were counted as a percentage of total cells. Detached cells from the media and adherent cells were both counted for accurate measurement. Cells were not split or fed (0 to 72 hours) following the replacement of the ATMi-containing medium with fresh medium at 1 hour. We did not observe an increase in cell death with increased concentration of ATMi (**figure 3.7B**). Total live cell percentage does not drop below 85%. We therefore used the ATMi concentrations and time points studied in this experiment for further investigations.

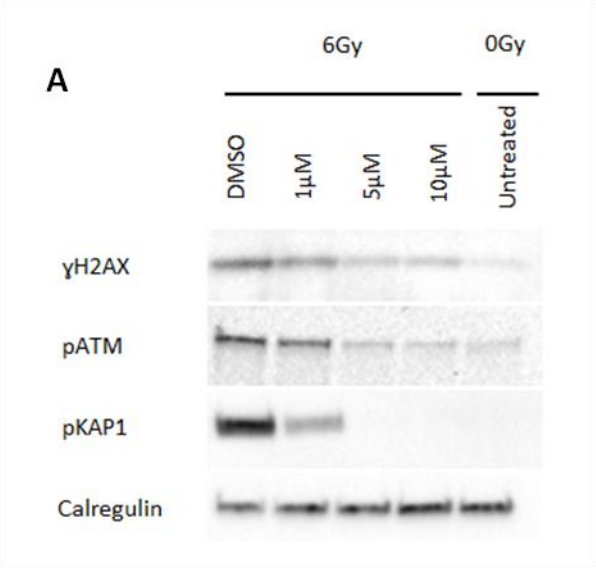


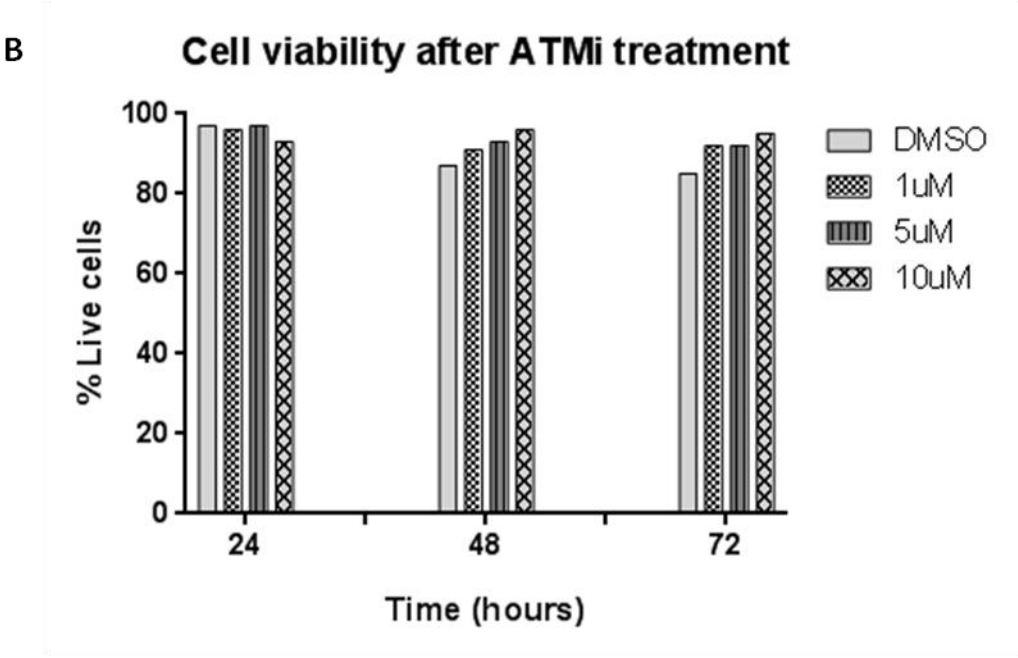


**Figure 3.7 Efficiency and toxicity of ATMi KU55933. A)** 293 cells were treated with various concentrations of ATMi: 0µM (DMSO-only), 1µM, 5µM or 10µM. After 1 hour, cells were treated with 6Gy radiation and harvested after a further one hour. Western blot analysis was used to determine phosphorylation levels of appropriate ATM targets. **B)** The cells were treated as above, then viability was assessed using Trypan Blue. The percentage of live cells was recorded at 0hrs, 24hrs, 48hrs and 72hrs.

We then investigated if the inhibition of ATM would alter the levels of EBV lytic gene transcripts. 2089 cells were treated with ATMi for 1 hour then induced into lytic cycle by transfection of BZLF1. The cells were harvested every 24 hours over 3 days, cDNA generated and qPCR performed using a 48:48 Dynamic Array IFC as described in materials and methods. All samples were measured in duplicate (standard deviations shown as error bars) with the exception of the 72 hour DMSO-only sample. The original experimental design was to normalise the transcript data in comparison to one of the housekeeping genes PGK1, GAPDH or B2M. However this proved not to be possible due to the unexpected reduction of the expression of housekeeping genes over time (**figure 3.8**) possibly due to virally induced shut off of host cell protein synthesis. Instead data shown in this section have been presented as transcripts per µL of RNA.

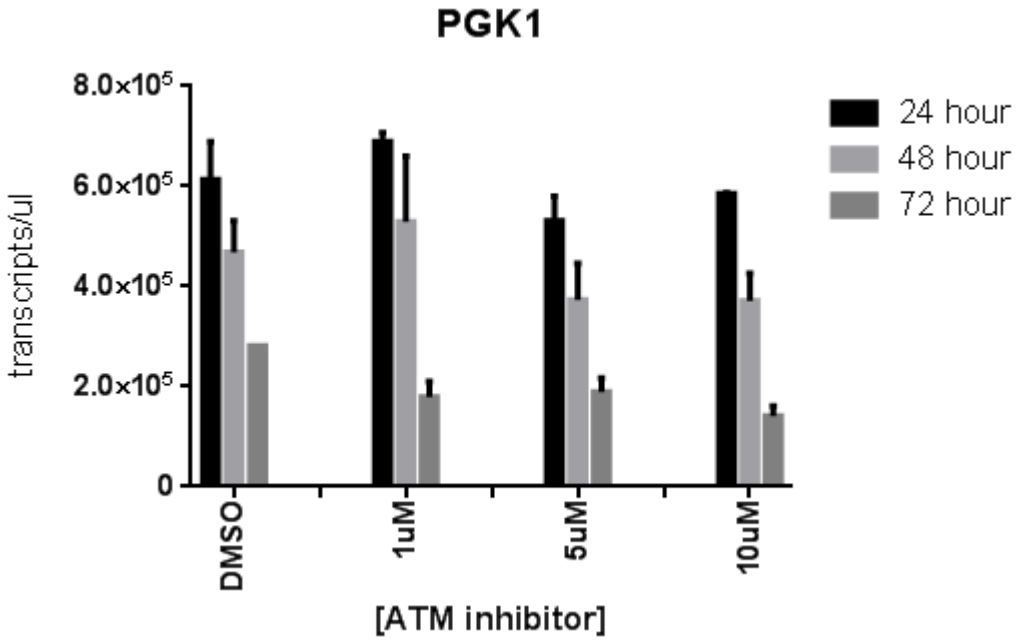


**Figure 3.8 Transcript levels of PGK1 during lytic induction and ATMi.** 2089 cells were induced into lytic replication after ATMi treatment and harvested for qPCR analysis of generated cDNA. PGK1, shown here, is representative of the trend observed with the housekeeping genes.

EBV transcript levels were analysed with the same samples (**figure 3.12**). Transcripts of all EBV genes increases over time as expected due to the continual expression of BZLF1. BZLF1 expression is shown in **figure 3.9A**. Very little difference is seen between BZLF1 expression at 24 hours with DMSO, 1μM and 5μM samples. However there is then a 5-fold increase from 5μM to 10μM at this time point. At later time points, lower concentrations of the ATMi seem to have an effect on BZLF1 transcript levels. The three test concentrations of the ATMi have comparable results of around 2.5 to 3-fold increase relative to the DMSO-only sample. The 48 hour samples show a distinct pattern in between the other time points because in this case the major increase in transcript level seems to occur between 1μM and 5μM. Here we see a 6-fold increase in number of transcripts per μL.

Transcriptional analysis of the other immediate early gene, BRLF1, is shown in (**figure 3.9B**) and showed a significantly lower level of expression than BZLF1, probably due to the fact the BZLF1 gene is overexpressed as it has been transfected into the cells using a plasmid vector. The two major trends are similar to that observed for BZLF1: expression increases over time and expression increases with higher concentrations of ATMi. The changes are noticeably more gradual with 0 to 2-fold differences between each time point at each concentration. Slight changes are also apparent for BHRF1 expression (**figure 3.9C**) where there is a great increase from 48 hours to 72 hours in gene expression; however, this is also seen in the DMSO control and not attributable to the inhibitor.

Changes in gene expression level for BMLF1 (**figure 3.9D**) and BMRF1 (**figure 3.9E**) are minimal and comparable data points are not significantly different from each other. BMLF1 expression at 72 hours appears abnormally low considering the two major trends throughout these results but this is likely to be an anomaly. BALF1 (**figure 3.9F**), BALF2 (**figure 3.9G**) and BGLF5 (**figure 3.9H**) show very little expression at 24 hours at all ATMi concentrations but there is a 3-fold change from DMSO control to 10μM.

GP350 was also analysed to determine whether structural genes were undergoing the same pattern as the immediate early and early gene transcripts (**figure 3.9I**). At 24 hours, there seems to be low levels of expression of this late gene but this was still surprisingly high when compared to certain early genes such as BALF1. The two major trends also applied here but only less than 2-fold changes were seen at any comparable data points across the different concentrations.

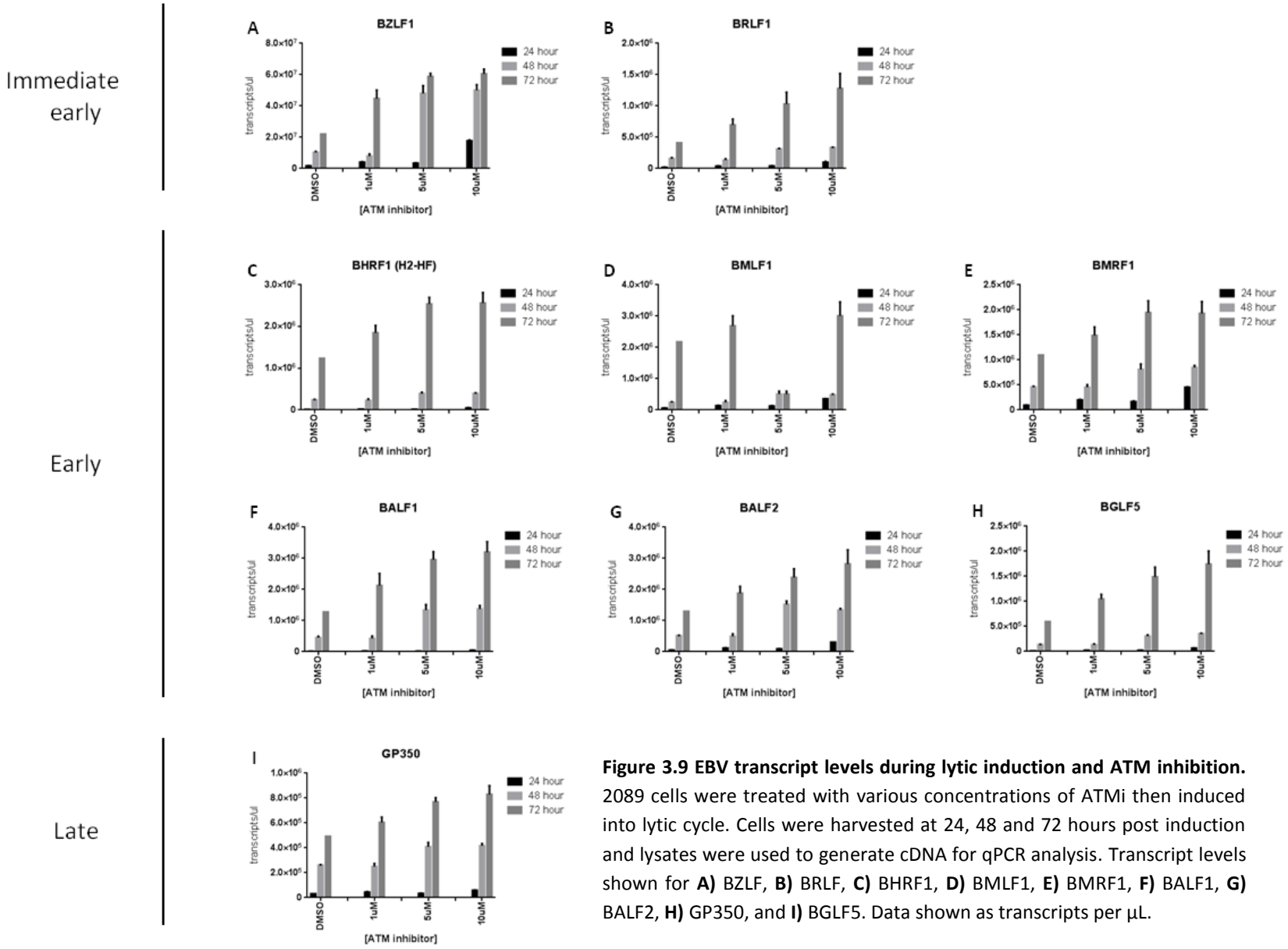


**Figure 3.9 EBV transcript levels during lytic induction and ATM inhibition.** 2089 cells were treated with various concentrations of ATMi then induced into lytic cycle. Cells were harvested at 24, 48 and 72 hours post induction and lysates were used to generate cDNA for qPCR analysis. Transcript levels shown for **A)** BZLF, **B)** BRLF, **C)** BHRF1, **D)** BMLF1, **E)** BMRF1, **F)** BALF1, **G)** BALF2, **H)** GP350, and **I)** BGLF5. Data shown as transcripts per µL.

### 3.5 Activity of the viral kinase, BGLF4, during lytic replication

The virally encoded kinase, BGLF4, has previously been reported to be involved in inducing a DNA damage response by indirectly activating ATM. In order to examine possible interactions between BLGF4 and cellular damage proteins, we performed a co-IP experiment (**figure 3.10**). 2089 cells were induced into lytic cycle and harvested at 24 hours post induction. A no-antibody sample and 293 lysate (10µg) were used as negative and positive controls respectively. No clear bands are visible in the IP lanes for Mre11 or Rad50 relative to the negative control suggesting no BGLF4 interaction has occurred with these proteins. An apparent RPA band was observed with the immunoprecipitated BGLF4 although it has run at a higher molecular weight than the RPA in the 293 lysate control. Distinct staining has occurred at the right sizes for both p53 and NBS1 in the test IP samples.

Given the apparent interaction between BGLF4 and certain DDR proteins, we decided to further investigate the viral kinase by immunofluorescence microscopy. 2089 cells were induced into lytic cycle by the transfection of BZLF1, plated on to chamber-well slides and fixed at 24 hours. The cells were then co-stained with antibodies against BZLF1 and BGLF4 in order to see if BGLF4 was located at replication compartments. The staining results shown in **figure 3.11** are representative of the cells in lytic cycle and show a distinct pattern of BGLF4 staining adjacent to, and outside, the nucleus. BGLF4 appears not to co-localise with BZLF1 within the nucleus as is known to be the case with other lytic proteins. Furthermore, not all lytic cells are showing this specific BGLF4 staining pattern and most lytic cells are not showing any BGLF4 staining at all. The BGLF4 staining can also be observed in distinct foci and concentrated in one generalised area within the cell.

Immunofluorescence staining prompted us to investigate whether BGLF4 was being exported from the nucleus during lytic cycle or if the antibody used was non-specific. Initially, BGLF4-KO cells were induced into lytic cycle by BZLF1 transfection, grown on chamber-well slides, fixed after 24 hours and stained for both BZLF1 and BGLF4. The same staining pattern was observed as in our BGLF4-KO cells

and the 2089 cells (data not shown) therefore the antibody is not suitable for immunofluorescence detection of BGLF4. We also tested the suitability of the antibody to detect BGLF4 in Western blot. EBV negative 293 cells were transfected with BGLF4 (HA tag) expression vector and harvested at 0, 24 and 48 hours. The samples were subjected to Western blot analysis and probed with BGLF4 and HA antibodies and a band was seen at approximately 48kDa, the reported size of the BGLF4 protein (**figure 3.12**). Bands were detected using the BGLF4 antibody at the correct size and only in the 24 and 48 hour samples suggesting the antibody is specific to BGLF4 for Western blot. Detection of HA at the same size confirmed this finding. However, unexpectedly, BGLF4 was not detected at 48kDa within the 2089 cells at the same time points even with long exposure. Although we cannot confirm the presence of BGLF4 in 2089 cells with an alternative antibody at this time, the data here could suggest BGLF4 cleavage due the presence of a strongly-staining band at lower molecular weight (unpublished observation by J. Zuo). As expected, no BGLF4 was detected in BGLF4-KO cells.

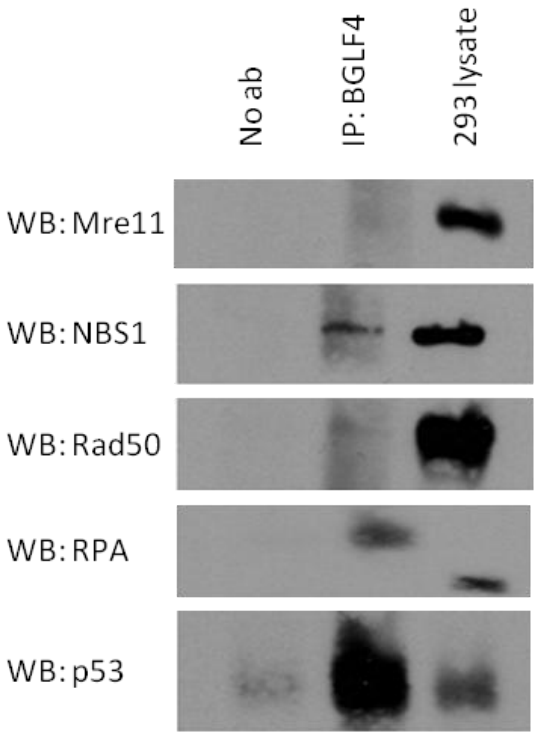


**Figure 3.10 Co-immunoprecipitation for the interaction between BGLF4 and DDR proteins.** 2089 cells induced into lytic cycle by transfection of p509 (BZLF1) and harvested at 24 hours. Antibody against BGLF4 was used to IP followed by Western blot analysis. 293 lysate was used as a positive control.

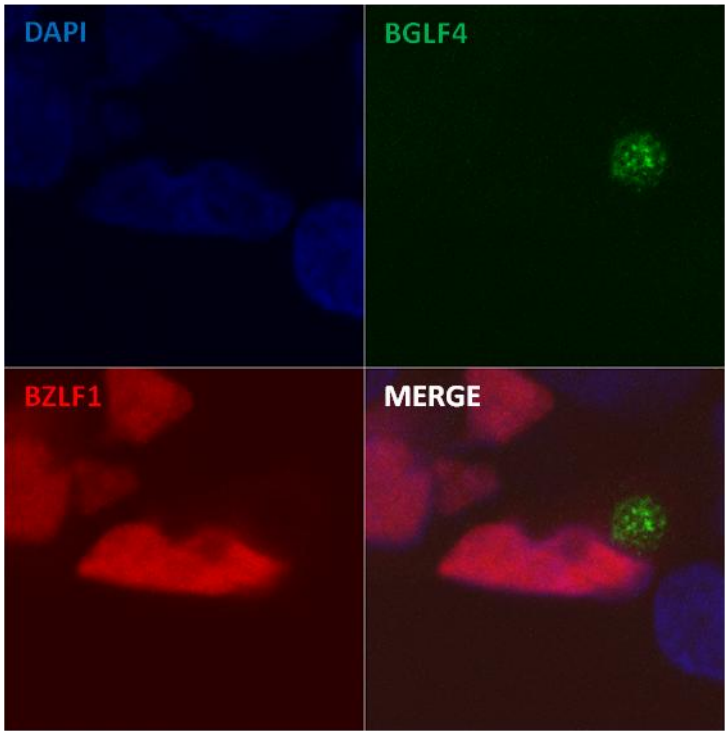


**Figure 3.11 Immunofluorescence staining of BGLF4 and BZLF1.** 2089 cells induced into lytic cycle by transfection of BZLF1 and fixed at 24 hours. The cells were stained for BGLF4 and BZLF1. Shown are representative micrographs of BGLF4-BZLF1 staining in one cell.

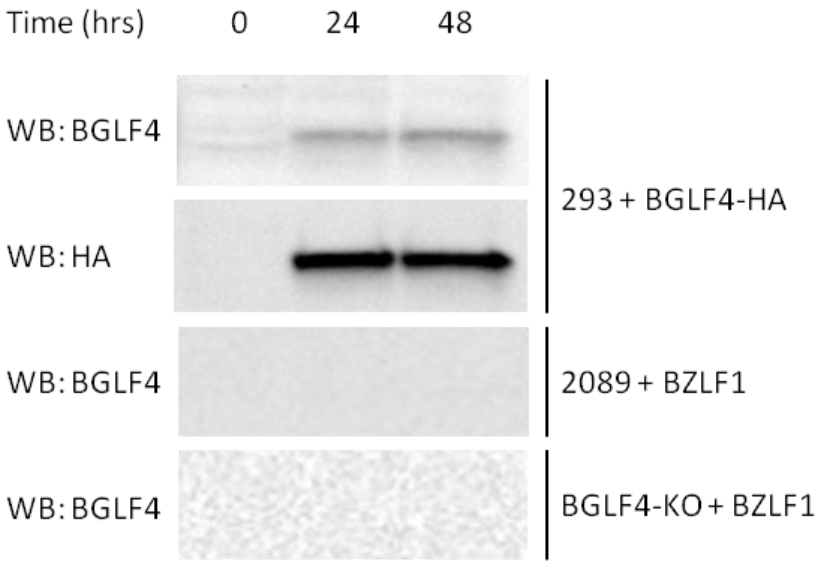


**Figure 3.12 Detection of BGLF4.** 293 cells were transfected with a BGLF4 gene encoding plasmid with an HA tag. 2089 cells and BGLF4-KO cells were induced into lytic cycle by transfection of BZLF1 and also harvested at the same points. Samples were harvested at the indicated time points and analysed by Western blot using antibodies against HA and BGLF4.

# 4. DISCUSSION

## 4.1 The dynamics of EBV lytic replication

In this project, we originally set out to examine if EBV utilized the DDR proteins to help replicate the viral genome efficiently, as seen in several different viruses including adenovirus, herpes simplex virus and polyomaviruses (reviewed by Turnell and Grand, 2012). Our chosen model to examine this question was primary differentiated tonsillar epithelial cells because EBV is naturally lytic in these cells (Feederle et al, 2007). The major advantage of this model is that cells do not require artificial lytic cycle induction techniques, for instance chemical induction (e.g.5-azacytidine and sodium butyrate). We confirmed that the viral lytic cycle was indeed induced in these cells immediately following EBV infection (**figure 3.1C**). However, due to circumstances beyond our control, including difficulty in obtaining the tonsils in a timely manner, bacterial infection and dramatic loss of cells during fluorescently activated cell sorting (FACS), we were unable to obtain further meaningful results with the primary epithelium.

The gene expression pattern in the infection of primary differentiated tonsillar epithelial cells varies greatly from our 2089 model of lytic replication. 2089 cells require the transfection of a BZLF1 expression vector leading to the over-expression of BZLF1 protein which continues to activate downstream lytic gene promoters. This is why we see a continual increase in lytic gene expression over time whereas our primary cell infections undergo a much earlier and shorter lytic event which peaks possibly even earlier than 24 hours post infection. Considering the immunofluorescence at the single cell level, we see a very dynamic process. Despite all cells being fixed at 24 hours post induction, it is not necessarily true that all transfected cells begin lytic cycle synchronously. This is exemplified by the pan-nuclear staining seen in **figures 3.4 and 3.5** in certain panels, compared to the punctate staining seen in others, which are probably images taken slightly before or after the

formation of replication compartments. It is also worth noting that not all induced cells will undergo complete lytic cycle i.e. only expressing some lytic proteins but not all (data not shown) which brings uncertainty to EBV and DDR co-localisation studies.

### 4.2 The requirement for the DNA damage response during lytic cycle

The recruitment of HR proteins to EBV replication compartments has been reported and speculated to be involved in the repair of viral DNA following damage. In 2009, Kudoh et al showed the co-localisation of Mre11, Nbs1 and Rad51 with the early viral proteins BALF2 and BMRF1. They also showed that RPA, whilst phosphorylated at its DNA damage associated sites, localised to the same sites within the nucleus to interact with BMRF1. This work followed the observation that both p53 and ATM associated with viral replication compartments in a latently infected marmoset B cell line (Kudoh et al, 2005). This evidence was reinforced by the binding of pRPA and Mre11 to the BALF5 gene and the BZLF1 promoter detected by chromatin-immunoprecipitation.

We set out to examine the ability of EBV to induce a DDR to assist its replication during lytic cycle in a human cell line. However, this could not be determined due to the activation of the DDR following transfection of foreign viral DNA in our control. This makes the data difficult to interpret and we are unable to determine whether the response observed is induced in any way by the direct action of viral lytic proteins. We also observed phosphorylation of CHK2 at 0 hours before any transfection has been carried out. This indicates an inappropriate damage response is occurring with no stimuli; possibly due to the model we are using as 293 cells are transformed by adenovirus E1 region with E1A and E1B proteins constitutively expressed. AdE1A and AdE1B55K have known involvement with the DDR, for example, being responsible for the up-regulation of p53 expression. A key difference is the phosphorylation of Nbs1 in the control cells not present in our lytic cells suggesting that the virus is possibly preventing the activation of the MRN complex. ATM targets p53, CHK2, H2AX and ATM

itself have been shown to be phosphorylated within 48 hours of EBV lytic reactivation, but again in a marmoset system. Interestingly, this study also showed a lack of ATR target activation (i.e. no CHK1 phosphorylation).

We hypothesised that components of the DDR would co-localise with viral proteins within replication compartments in our human 2089 model based upon current understanding of the relationship. We therefore optimized the antibodies for the proteins we chose to examine on gamma-irradiated cells to ensure the formation of damage foci could be differentiated from background expression. Co-localisation was largely unseen in our experiments with the notable exception of pRPA. Despite its failure to interact with BMRF1 and BALF2 in our co-IP assays, it still may be loaded onto newly synthesised viral DNA as suggested in previous reports (Kudoh et al, 2009). The problem here may be due to an insufficient level of interaction between the two proteins at 24 hours but even over-expression of the viral proteins in 293 proteins yielded the same result. However, an interaction between the viral mRNA export factor (BMLF1) and RPA is indicated by our data (**figure 3.6D**) but this will need to be verified by a co-IP with the reverse antibody. We showed phosphorylation of ATM but failed to show clear co-localisation at viral replication centres but most surprisingly there appeared to be little foci recruitment for Rad50 or Rad51. The data here suggests that EBV is not using cellular repair proteins during lytic cycle but there is a strong relationship with RPA. SV40 is known to utilise RPA, via large T antigen, in order to replicate its DNA (Melendy and Stillman, 1998). The increasing presence of RPA correlates to increases in levels of SV40 DNA replication (Wang et al, 2000). As RPA has multiple functions, it could be involved with a DNA replication function rather than DNA repair in the context of EBV based on the observation made here. This theory is supported by the lack of ATR substrate activation in previous studies described above.

EBV lytic reactivation, in certain latently infected cell lines, can occur by various methods such as radiation and chemotherapy agents both of which are DDR inducing stimuli (Westphal et al, 2002;

Feng et al, 2000). It has been proposed that EBV lytic reactivation is a p53 dependent event in epithelial cell lines (Hagemeier et al, 2011). However, it also been shown that p53 is tagged by ubiquitin for proteasome mediated degradation induced by BZLF1 so the relationship is not obvious (Sato et al, 2009). The function of another central DDR kinase, ATM, is also under investigation for its involvement in EBV lytic cycle. Previous studies report that ATM inhibition (or treatment with the exogenous indirect ATM activator Nutlin-3) leads to the inhibition of EBV lytic gene expression except, notably, in p53 negative cell lines (Hagemeier, 2012). The same group also showed in 2089 cells that ATM inhibition did not prevent BZLF1 expression. To follow on from this, we carried out these experiments to quantify the level of lytic gene transcripts at various time points and ATMi concentrations in order to further understand the relationship. Our data agrees that ATM inhibition in 2089 cells does not prevent BZLF1 expression but surprisingly, ATM appeared to be inhibitory to lytic gene expression. We stipulate this because with increasing concentrations of ATMi, greater lytic gene transcription occurs (**figure 3.9**). As the expression of genes downstream of BZLF1 correlate with BZLF1 expression (although to different extents), we believe this is not a result of direct action, or lack of action, by ATM. Hagemeier et al suggest that 2089 is a special circumstance as the expression vector-mediated BZLF1 overcomes the need for ATM to activate its promoter relative to other cell lines with chemically induced lytic reactivation. However, the trend in our data behaves as if a down-regulator of BZLF1 expression has been removed which is not explained by that theory. In 2089 cells, BZLF1-mediated degradation of p53 has been shown to be important for viral lytic cycle due to the capability of p53 to initiate apoptosis (Sato et al, 2009). Our data could be an extension of this as ATM targets p53 for downstream activation (which includes the possibility of apoptosis). The apparent increase in lytic gene transcripts with increasing concentration of ATMi over time could be a result of more cells surviving the course of the experiment due to less cells undergoing p53-induced apoptosis.

### 4.3 Potential implications for LETM1 and BALF2 function

LETM1 is a $H^+$-$Ca^{2+}$ exchanger that functions at the inner mitochondrial membrane and contributes to the control of $Ca^{2+}$ influx into mitochondria. Knockout of LETM1 in transgenic mice causes deregulated glucose and ATP levels when not lethal (Jiang et al, 2013). The LETM1 gene is also known to be deleted in Wolf-Hirschhorn syndrome (Bergemann et al, 2005). High $Ca^{2+}$ levels within the mitochondria lead to the opening of a permeability transition pore (PTP). Pro-apoptotic factors such as cytochrome c that induce apoptosome formation are released through the PTP. A virus undergoing lytic cycle is exposing much more of its genome than in its latent cycle and the cell is therefore much more likely to initiate apoptosis. One reason for this is that lytic proteins are highly susceptible to antigen processing and presentation on surface MHC molecules to surveying CD4+ T cells which induce apoptosis by death receptor signalling. The virus needs to combat this in order to replicate itself and release new virions from the infected cell. EBV encodes a protein, which is highly efficient at inhibiting apoptosis; BHRF1, a viral Bcl2 homologue. We have shown BALF2 to interact with LETM1 during viral lytic cycle in our 2089 cell model. It is therefore possible that BALF2 is interacting with LETM1 in order to reduce the influx of $Ca^{2+}$ into the mitochondria to prevent the release of pro-apoptotic factors in order to allow virion production. This would be unusual due to the currently understood function of BALF2 as a DNA binding protein but viral proteins are known for their multifunctional nature. This certainly warrants further investigation.

Wolf-Hirschhorn syndrome (WHS) is defined by a deletion in the short arm of chromosome 4 leading to the loss of the WHS critical region which includes the LETM1 and WHSC1 (Wolf-Hirschhorn syndrome candidate 1) genes (Bergemann et al, 2005; Hajdu et al, 2011). Clinical presentations of WHS include immunodeficiency, developmental defects and microcephaly. Some of these symptoms are shared with ataxia telangiectasia (A-T) patients, a condition characterised by mutation of the ATM gene (Biton et al, 2008). It has been shown that WHSC1 is involved in the DDR with its recruitment to sites of DNA damage induced by UV radiation and requirement for CHK2 activation

(Bergemann et al, 2005). LETM1 may also have an unknown function in the DDR due to its contribution towards the pathogenesis of WHS when absent. Although our data here does not strongly suggest BALF2 is involved with the DDR, other reports have done so. The BALF2 and LETM1 interaction we report could indicate a role for LETM1 in the DNA damage response.

### 4.4 The role of BGLF4 during lytic cycle

BGLF4 has known involvement with the cellular DDR hence its initial investigation for binding partners (Li et al, 2011). The MRN complex was chosen for co-IP investigation with BGLF4 as a potential target for phosphorylation. Nbs1 appears to interact with BGLF4 which is surprising considering data generated in **figure 3.2** which suggests Nbs1 phosphorylation was being inhibited during lytic cycle. BGLF4 could be responsible for the phosphorylation of RPA as an interaction between the two proteins was observed. Again unexpectedly, our data suggests BGLF4 is targeting p53 despite previous studies suggesting p53 is degraded in this model of lytic replication. BGLF4 is known to phosphorylate BZLF1 hence why it was co-stained with the BZLF1 protein but unexpectedly, we did not see any co-localisation. We expect to see the lytic protein within the nucleus along with its partners as these are genes associated with viral DNA replication and viral DNA packaging. The specificity of the antibody is not wholly trusted. BGLF4 cleavage within the context of lytic cycle is a possibility based on **figure 3.12**. BGLF4 is shown at its theoretical molecular weight therefore it is probable that another viral protein is responsible for its cleavage which does not occur in EBV negative 293 cells transfected with BGLF4. These findings are novel and have implications on the interpretation of published data.

### 4.6 Conclusions and future work

The dynamics of EBV lytic gene expression in the 2089 cell line differs greatly from a more physiologically appropriate model in primary keratinocytes. EBV replication is an earlier and quicker process than the 2089 model indicates. 2089 cells also generate a DDR after transfection of foreign DNA clouding any detectable DDR induction by viral lytic proteins. The ATR target RPA is associated with EBV replication compartments within the cellular nucleus but may only be involved in a DNA replication role rather than repair. ATR inhibition could prove insightful. Previous studies showed that ATM, Rad50 and Rad51 locate with viral proteins during lytic replication but our model failed to reproduce this result. As only a select few out of the numerous DDR proteins have been investigated, further co-localisation studies need to be carried out before final conclusions can be made. ATM activity is either inhibitory to EBV lytic gene expression or works to induce apoptosis preventing viral replication. Collectively, the data presented here suggests that EBV does not rely on ATM or its downstream targets to replicate its DNA but does perhaps need the ATR target RPA. The differences we see here are due to either one of two possibilities. The first being the abnormal DDR pathways in 293 cells, due to their method of transformation into a cell line, has affected the way in which the virus can interact with it. The second is that previous studies have been largely carried out on marmoset cell line containing the B95.8 clone of EBV. We have to be wary of using human antibodies on cell lines from other species and interpreting their meaning. Although the different cell lineages might express differing DNA damage expression patterns which may contribute to differing immunofluorescence imaging.

BGLF4 is possibly cleaved during lytic cycle by a viral protein either directly or indirectly but a candidate is not apparent at present. Such proteolysis is seen with various cellular enzymes as an activating mechanism which is a theory that might be appropriate here but the data is preliminary. The interaction between BALF2 with LETM1 indicates a novel function for the viral DNA binding protein in the regulation of apoptosis if this result can be verified. Ideally, investigation will move to a

primary differentiated epithelial cell or plasma cell background for more conclusive data towards answering key questions in EBV virology.

## 5. REREFENCES

**Babcock GJ, Decker LL, Volk M, and Thorley-Lawson DA. (1998).** EBV persistence in memory B cells in vivo. Immunity. 9:395–404.

**Bergemann AD, Cole F and Hirschhorn K. (1999).** The etiology of Wolf-Hirschhorn syndrome. *Trends Genet.* 21(3):188-95.

**Biton S, Barzilai A and Shiloh Y. (2008).** The neurological phenotype of ataxia-telangiectasia: Solving a persistent puzzle. *DNA repair.* 7:1028-38.

**Blackford AN and Grand RJ. (2009).** Adenovirus E1B 55-kilodalton protein: multiple roles in viral infection and cell transformation. *J Virol.* 83(9):4000-12.

**Buisson M, Hans F, Kusters I, Duran N, Sergeant A. (1999).** The C-terminal region but not the Arg-X-Pro repeat of Epstein-Barr virus protein EB2 is required for its effect on RNA splicing and transport. *J Virol.* 73(5):4090-100.

**Burma S and Chen DJ. (2004).** Role of DNA-PK in the cellular response to DNA double-strand breaks. *DNA Repair*. 3(8-9):909-18.

**Chen YR, Liu MT, Chang YT, Wu CC, Hu CY and Chen JY. (2008).** Epstein-Barr virus latent membrane protein 1 represses DNA repair through the PI3K/Akt/FOXO3a pathway in human epithelial cells. *J Virol.* 82(16):8124-37.

**Cimprich KA and Cortez D. (2008).** ATR: an essential regulator of genome integrity. *Nat Rev Mol Cell Biol.* 9(8):616-27.

**Dahl J, You J, Benjamin TL. (2005).** Induction and utilization of an ATM signaling pathway by polyomavirus. *J Virol.* 79(20):13007-17.

**Daikoku T, Kudoh A, Fujita M, Sugaya Y, Isomura H, Shirata N and Tsurumi T. (2005).** Architecture of Replication Compartments Formed during Epstein-Barr Virus Lytic Replication. J Virol. 79(6):3409-3418.

**Derheimer FA and Kastan MB. (2010).** Multiple roles of ATM in monitoring and maintaining DNA integrity. *FEBS Lett.* 584(17):3675-3681.

**Epstein MA, Barr YM and Achong BG. (1964).** Virus particles in cultured lymphoblasts from Burkitt's lymphoma. *Lancet.* 15:702–703.

**Erickson KD, Bouchet-Marquis C, Heiser K, Szomolanyi-Tsuda E, Mishra R, Lamothe B, Hoenger A and Garcea RL. (2012).** Virion Assembly Factories in the Nucleus of Polyomavirus-Infected Cells. *PLoS Pathog.* 8(4):E1002630.

**Feederle R, Neuhierl B, Bannert H, Geletneky K, Shannon-Lowe C and Delecluse HJ. (2007).** Epstein-Barr virus B95.8 produced in 293 cells shows marked tropism for differentiated primary epithelial cells and reveals interindividual variation in susceptibility to viral infection. *Int J Cancer.* 121(3):588-94.

**Feng WH, Israel B, Raab-Traub N, Busson P and Kenney SC. (2002).** Chemotherapy induces lytic EBV replication and confers ganciclovir susceptibility to EBV-positive epithelial cell tumors. *Cancer Res.* 62(6):1920-6.

**Hagemeier SR1, Barlow EA, Kleman AA and Kenney SC. (2011).** The Epstein-Barr virus BRRF1 protein, Na, induces lytic infection in a TRAF2- and p53-dependent manner. *J Virol.* 85(9):4318-29.

**Hagemeier SR, Barlow EA, Meng Q and Kenney SC. (2012).** The cellular ataxia telangiectasia-mutated kinase promotes epstein-barr virus lytic reactivation in response to multiple different types of lytic reactivation-inducing stimuli. *J Virol.* 86(24):13360-70.

**Hajdu I, Ciccia A, Lewis SM and Elledge SJ. (2011).** Wolf–Hirschhorn syndrome candidate 1 is involved in the cellular response to DNA damage. *Proc Natl Acad Sci.* 108(32):13130-34.

**Jackson SP and Barteck J. (2009).** The DNA damage response in human biology and disease. *Nature*. 461:1071-1078.

**Jiang D, Zhao L, Clish CB and Clapham DE. (2013).** Letm1, the mitochondrial Ca2+/H+ antiporter, is essential for normal glucose metabolism and alters brain function in Wolf-Hirschhorn syndrome. *Proc Natl Acad Sci.* 110(24):2249-54.

**Kawanishi S, Hiraku Y, Pinlaor S and Ma N. (2006)** Oxidative and nitrative DNA damage in animals and patients with inflammatory diseases in relation to inflammation-related carcinogenesis. *Biol Chem.* 387(4):365-72.

**Kudoh A, Fujita M, Zhang L, Shirata N, Daikoku T, Sugaya Y, Isomura H, Nishiyama Y and Tsurumi T. (2005).** Epstein-Barr virus lytic replication elicits ATM checkpoint signal transduction while providing an S-phase-like cellular environment. *J Biol Chem.* 280:8156–8163.

**Kudoh A, Iwahori S, Sato Y, Nakayama S, Isomura H, Murata H and Tsurumi T. (2009).** Homologous recombinational repair factors are recruited and loaded onto the viral DNA genome in Epstein-Barr virus replication compartments. *J Virol.* 83(13):6641-51.

**Laichalk LL and Thorley-Lawson DA. (2005).** Terminal Differentiation into Plasma Cells Initiates the Replicative Cycle of Epstein-Barr Virus In Vivo. *J Virol.* 79(2):1296-307.

**Li R, Zhu J, Xie Z, Liao G, Liu J, Chen MR, Hu S, Woodard C, Lin J, Taverna SD, Desai P, Ambinder RF, Hayward GS, Qian J, Zhu H and Hayward SD. (2011).** Conserved herpesvirus kinases target the DNA damage response pathway and TIP60 histone acetyltransferase to promote virus replication. *Cell Host Microbe.* 10:390-400.

**Liu P and Speck SH. (2003).** Synergistic autoactivation of the Epstein-Barr virus immediate-early BRLF1 promoter by Rta and Zta. *Virology*. 310(2):199-206.

**Melendy T and Stillman B. (1993).** An interaction between replication protein A and SV40 T antigen appears essential for primosome assembly during SV40 DNA replication. *J Biol Chem.* 268(5):3389-95.

**Moody CA and Laimins LA. (2009).** Human Papillomaviruses Activate the ATM DNA Damage Pathway for Viral Genome Amplification upon Differentiation. *Plos Patogh.* 5(10):E1000605.

**Nemerow GR, Mold C, Schwend VK, Tollefson V and Cooper NR. (1987)** Identification of gp350 as the viral glycoprotein mediating attachment of Epstein–Barr virus (EBV) to the EBV/C3d receptor of B cells: sequence homology of gp350 and C3 complment fragment C3d. J. Virol. 61:1416–1420.

**Nikitin PA, Yan CM, Forte E, Bocedi A, Tourigny JP, White RE, Allday MJ, Patel A, Dave SS, Kim W, Hu K, Guo J, Tainter D, Rusyn E and Luftig MA. (2010).** An ATM/Chk2-mediated DNA damage-responsive signaling pathway suppresses Epstein-Barr virus transformation of primary human B cells. *Cell Host Microbe.* 8(6):510-22.

**Rickinson AB and Kieff E. (2001).** *Fields Virology*. 4th edn. Knipe DM and Howley PM (eds). Lippincott Williams & Wilkins Publishers: Philadelphia, pp. 2575–2627.

**Rooney CM, Rowe DT, Ragot T and Farrell PJ. (1989).** The spliced BZLF1 gene of Epstein-Barr virus (EBV) transactivates an early EBV promoter and induces the virus productive cycle. *J. Virol.* 63:3109-3116.

**Sato Y, Kamura T, Shirata N, Murata T, Kudoh A, Iwahori S, Nakayama S, Isomura H, Nishiyama Y, Tsurumi T. (2009a).** Degradation of phosphorylated p53 by viral protein-ECS E3 ligase complex. *PLoS Path*. 5(7):E1000530.

**Shannon-Lowe C and Rowe M. (2011).** Epstein-Barr virus infection of polarized epithelial cells via the basolateral surface by memory B cell-mediated transfer infection. *PLoS Pathog.* 7(5):E1001338.

**Shirata N, Kudoh A, Daikoku T, Tatsumi Y, Fujita M, Kiyono T, Sugaya Y, Isomura H, Ishizaki K and Tsurumi T. (2005).** Activation of ataxia telangiectasia-mutated DNA damage checkpoint signal transduction elicited by herpes simplex virus infection. *J Biol Chem*. 280(34):30336-41.

**Slobedman B, Barry PA, Spencer JV, Avdic S and Abendroth A. (2009).** Virus-Encoded Homologs of Cellular Interleukin-10 and Their Control of Host Immune Function. *J Virol.* 83(19):9618-29.

**Stracker TH, Carson CT and Weitzman MD. (2002).** Adenovirus oncoproteins inactivate the Mre11-Rad50-NBS1 DNA repair complex. *Nature*. 418(6895):348-52.

**Szekely L, Selivanova G, Magnusson K, Klein G and Wiman KG. (1995)** EBNA-5, Epstein-Barr encoded nuclear antigen, binds to the retinoblastoma and p53 proteins. *Proc Natl Acad Sci.* 90:5455–5459.

**Taub R, Kirsch I, Morton C, Lenoir G, Swan D, Tronick S, Aaronson S and Leder P. (1982)** Translocation of the c-myc gene into the immunoglobulin heavy chain locus in human Burkitt lymphoma and mouse plasmacytoma cells. *Proc Natl Acad Sci.* 79:7837–7841.

**Thompson MP and Kurzrock R. (2004).** Epstein-Barr Virus and Cancer. *Clin Cancer Res.* 10:803-821.

**Turnell A and Grand RJ. (2012).** DNA viruses and the cellular DNA-damage response. *J Gen Virol.* 93:2076-97.

**Wang M, Parl JS, Ishiai M, Hurwitz J and Lee SG. (2000).** Species specificity of human RPA in simian virus 40 DNA replication lies in T-antigen-dependent RNA primer synthesis. *Nucleic Acids Res*. 28(23):4742-9.

**Ward JF. (1990).** The Yield of DNA Double-strand Breaks Produced Intracellularly by Ionizing Radiation: A Review. *Int J Radiat Biol.* 57(6):1141-50.

**Westphal EM, Blackstock W, Feng W, Israel B and Kenney SC. (2002).** Activation of lytic Epstein-Barr virus (EBV) infection by radiation and sodium butyrate in vitro and in vivo: a potential method for treating EBV-positive malignancies. *Cancer Res.* 60(20):5781-8.

**Zimber-Strobl U, Kempkes B, Marschall G, Ziedler R, Van Kooten C, Banchereau J, Bornkamm GW and Hammerschmidt W. (1996)** Epstein-Barr virus latent membrane protein (LMP1) is not sufficient to maintain proliferation of B cells but both it and activated CD40 can prolong their survival. *EMBO J.* 15: 7070–7078.

# 6. APPENDICES

## 6.1 Appendix I: AQ Plasmid

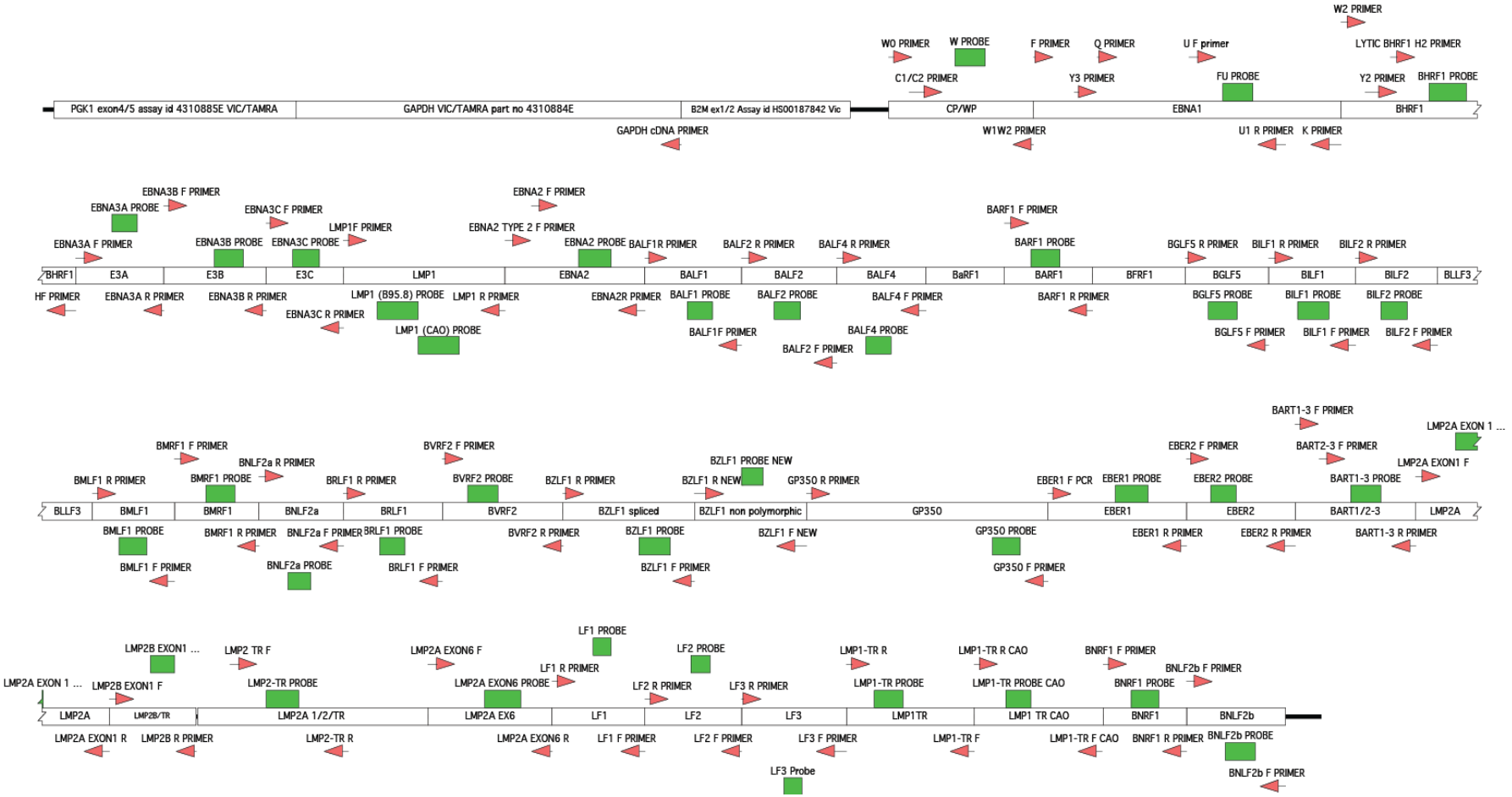

## 6.2 Appendix II: Primer sequences

| Assay | Primer/Probe | EBV genome coordinates * | Sequence | 20x conc. |
|---|---|---|---|---|
| Wp | W0 | 14391–14410 | CGCCAGGAGTCCACACAAAT | 2µM |
| | W1W2 | 14709–14701/ 14619–14612 | GAGGGGACCCTCTGGCC | 2µM |
| Cp | C1C2 | 11467–11479/ 11626–11639 | AATCATCTAAACCGACTGAAGAAACAG | 20µM |
| | W1W2 | 14709–14701/ 14619–14612 | GAGGGGACCCTCTGGCC | 20µM |
| Wp/Cp | W probe | 14564–14588 | ACCGAAGTGAAGGCCCTGGACCAAC | 10µM |
| | | | | |
| EBNA1 | Q | 62440–62456 | GTGCGCTACCGGATGGC | 20µM |
| | Y3 | 48422–48440 | TGCCTGAACCTGTGGTTGG | 20µM |
| | F primer | 50099-50115 | GGGTGAGGCCACGCTTT | 20µM |
| | U | 55247-55269 | CTGCAGCCCAGAGAGTAGTCTCA | 20µM |
| | U1 | 55326-55304 | CAGGTCTACTGGCGGTCTATGAT | |
| | K | 107952–107941/ 67649–67636 | CATGATTCACACTTAAAGGAGACGG | 20µM |
| | U probe | 67563–67587 | TCCTCTGGAGCCTGACCTGTGATCG | 10µM |
| | | | | |
| EBNA2 | EBNA2 Type1 F | 35702-35711 36098-36109/ | GCTTAGCCAGTAACCCAGCACT | 6 µM |
| | EBNA2 Type2 F | | GCTTAGCCAGTAACTCAGCGCT | 6 µM |
| | EBNA2 R | 36181-36160 | TGCTTAGAAGGTTGTTGGCATG | 6 µM |

| | | | | |
|---|---|---|---|---|
| | EBNA2 probe | 36127-36153 | CCCAACCACAGGTTCAGGCAAAACTTT | 10µM |
| | | | | |
| EBNA3A | EBNA3A F | 82313-82335 | CCCCTTAACTCAACCCATTAACC | 6 µM |
| | EBNA3A R | 81944-81929 | CGGCCCCTCCATTGGT | 6 µM |
| | EBNA3A probe | 82343-82363 | ACCCGCAGCCCATTTCCTCCA | 10µM |
| | | | | |
| EBNA3B | EBNA3B F | 83265-83281 | TGCCGCTGCAAGAGAGG | 20µM |
| | EBNA3B R | 83510-83500/ 83421-83413 | AGGTCCGATTGCAACATGGA | 20µM |
| | EBNA3B probe | 83347-83374 | CCTAGATTTGTGGATGTGAACCCAACGC | 10µM |
| | | | | |
| EBNA3C | EBNA3C F | 88813-88831 | TACGCCCCATTCCAACAAG | 6 µM |
| | EBNA3C R | 88876-88858 | CCCACGGCCATGCTATCTT | 6 µM |
| | EBNA3C probe | 88835-88856 | CCCCCCTCCCCCTATGCCGTTA | 10µM |
| | | | | |
| BHRF1 | W2 | 14810-14830 | TGGTAAGCGGTTCACCTTCAG | 6µM |
| | Y2 | 35706-35680 | GAGGATGAAGACTAAGTCACAGGCTTA | 6µM |
| | H2 | 41596-41607/ 42047-42055 | GGCTTACCTCGGTTCCCTCTT | 6µM |
| | HF | 42134-42111 | TCCCGTATACACAGGGCTAACAGT | 6µM |
| | Probe | 42067-42097 | TGCCAGATCTTGTAGAGCAAGATGGCCTATT | 10µM |
| | | | | |
| LMP1 | LMP1 F | 168644-168625 | AATTTGCACGGACAGGCATT | 6 µM |

| | | | | |
|---|---|---|---|---|
| | LMP1R | 168435-168454 | AAGGCCAAAAGCTGCCAGAT | 6 µM |
| | LMP 1 probe (B95) | 168951-168965/ 169042-169060 | TCCAGATACCTAAGACAAGTAAGCACCCGAAGAT | 10µM |
| | LMP1 probe (Cao) | | TCCAGAGACCTAAGACAAGTAAGCAGCCAAAGAT | 10µM |
| | | | | |
| LMP1-TR | LMP1-TR F (B95) | 169013-168994 | CCCCTCTCAAGGTCGTGTTC | 6 µM |
| | LMP1-TR F (Cao) | | GCGTCTCAAGGTCGCGTTC | 6 µM |
| | LMP1-TR R (B95) | 169099-169080 | CGTAGCCGCCCTACATAAGC | 6 µM |
| | LMP1-TR R (Cao) | | TCGTAGGCGGCCTACATAACC | 6 µM |
| | LMP1-TR probe (B95) | 169017-169040 | CCTCAGGGCAGTGTGTCAGGAGCA | 10µM |
| | LMP1-TR probe (Cao) | | TGCTCCTGCCACACTACCCTGACCA | 10µM |
| | | | | |
| LMP2 (total) | LMP2exon6 F | 1027-1049 | GGTTCTCCTGATTTGCTCTTCGT | 6 µM |
| | LMP2exon6 R | 1129-1113 | CGCGGAGGCTAGCAACA | 6 µM |
| | LMP2exon6 probe | 1074-1103 | TCCTTCTGGCACGACTGTTCCTATATGCTC | 10µM |
| | | | | |
| LMP2A | LMP2A exon1 F | 166109-166129 | TCCCTAGAAATGGTGCCAATG | 6 µM |
| | LMP2A | 166215- | GAAGAGCCAGAAGCAGATGGA | 6 µM |

| | | | | |
|---|---|---|---|---|
| | exon1 R | 166195 | | |
| | LMP2A probe | 166142-166160 | CCTAGCCCCGGCGGGGATC | 10µM |
| | | | | |
| LMP2B | LMP2B exon1F | 169365-169385 | GTAATCTGCACAAAGAGGCGC | 6 µM |
| | LMP2B exon1R | 169436-169421 | AAAGCACGGCCTCCCG | 6 µM |
| | LMP2B probe | 169399-169418 | TGCCGCCAACGACCTCCCAA | 10µM |
| | | | | |
| LMP2-TR | LMP2-TR F | 28-50 | ACTTTTCTTCTTGCCCGTTCTCT | 6 µM |
| | LMP2-TR R | 114-133 | GAAACACGAGGCGGCAATAG | 6 µM |
| | LMP2-TR probe | 66-92 | CAGTATGCCTGCCTGTAATTGTTGCGC | 10µM |
| | | | | |
| BZLF1 | BZLF1 F | 90859-90835 | CCCAAACTCGACTTCTGAAGATGTA | 20x |
| | BZLF1 R | 90767-90791 | TGATAGACTCTGGTAGCTTGGTCAA | custom |
| | BZLF1probe | 90803-90820 | CCCATACCAGGTGCCTTT | assay |
| | | | | |
| BRLF1 | BRLF1 F | 92662-92644 | TTGGGCCATTCTCCGAAAC | 6 µM |
| | BRLF1 R | 92581-92590 | TATAGGGCACGCGATGGAA | 6 µM |
| | BRLF1probe | 92611-92631 | AGACGGGCTGAGAATGCCGGC | 10µM |
| | | | | |
| BMLF1 | BMLF1 F | 71978-71958 | CCCGAACTAGCAGCATTTCCT | 6 µM |
| | BMLF1 R | 71805-71824 | GACCGCTTCGAGTTCCAGAA | 6 µM |
| | BMLF1 probe | 71941-71955 | AACGAGGATCCCGCAGAGAGCCA | 10µM |
| | | | | |

| | | | | |
|---|---|---|---|---|
| BALF1 | BALF1 F | 164694-169676 | GGGCAAAGACACGCACGTA | 6 µM |
| | BALF1 R | 164615-164633 | GCCGCGACCAGTAGTCGTA | 6 µM |
| | BALF1 probe | 164650-164670 | CATCATCAGCGTCCTGCGCGC | 10µM |
| | | | | |
| BALF2 | BALF2F | 164131-164113 | CGGGCTTCAGCATCAATGT | 6 µM |
| | BALF2R | 164053-164074 | TGATAGGAGGTAGCGCGTAGGA | 6 µM |
| | BALF2 probe | 164080-164101 | ACAGGAGGCCCGACCCCAACTG | 10µM |
| | | | | |
| BARF1 | BARF1 F | 165586-165606 | GGGAGCCTCTCTGTTGCTGTT | 6 µM |
| | BARF1 R | 165658-165639 | TTTTCCCAACGCAGGTCACT | 6 µM |
| | BARF1 probe | 165608-165631 | ACCTGTCACTTCCCAAGCCCTGGC | 10µM |
| | | | | |
| BGLF5 | BGLF5F | 108930-108913 | GCAAGCCCGGGAGAGACT | 6 µM |
| | BGFL5R | 108862-108879 | GAGGCGACCGTTTTCGAA | 6 µM |
| | BGLF5 probe | 108881-108904 | CGGGTGAACATTGTGACGGCCTTC | 10µM |
| | | | | |
| BHRF1 | H2 | 41596-41606/ 42047-42056 | GGCTTACCTCGGTTCCCTCTTA | 6 µM |
| | HF | 42111-42134 | TCCCGTATACACAGGGCTAACAGT | 6 µM |
| | BHRF1 probe | 42067-42097 | AATAGGCCATCTTGCTCTACAAGATCTGGCA | 10µM |

| | | | | |
|---|---|---|---|---|
| BMRF1 | BMRF1F | 68078-68098 | GAGGAACGAGCAGATGATTGG | 6 µM |
| | BMRF1R | 68147-68130 | TGCCCACTTCTGCAACGA | 6 µM |
| | BMRF1 probe | 68104-68127 | TGCTGTTGATGCCCAAGACGGCTT | 10µM |
| | | | | |
| BNLF2A | BNLF2A F | 167015-166996 | TGGAGCGTGCTTTGCTAGAG | 6 µM |
| | BNLF2A R | 166946-166966 | GGCCTGGTCTCCGTAGAAGAG | 6 µM |
| | BNLF2A probe | 166970-166988 | CCTCTGCCTGCGGCCTGCC | 10µM |
| | | | | |
| BNLF2B | BNLF2B F | 3482-3463 | GGAGTTTCCCCCGATTCAAG | 6 µM |
| | BNLF2B R | 166748-166769 | AAAGGTCAAAGAACAAGGCCAA | 6 µM |
| | BNLF2B probe | 166780-166804 | TCTGAAGGAACGGCGGAGAGTAGCG | 10µM |
| | | | | |
| BALF4 | BALF4F | 157766-157784 | CCTGGCCCTTCGTGTAACG | 20x |
| | BALF4R | 157835-157813 | GAAGAGCAGGTGAACAAGACCAT | custom |
| | BALF4probe | 157792-157807 | ACGGCCTCGTACTTCT | assay |
| | | | | |
| BILF1 | BILF1 F | 152353-152333 | TGCCTTTTGACCCAGAACATG | 6 µM |
| | BILF1 R | 152282-152303 | CAACGCCATACCCAAGTGAGT | 6 µM |
| | BILF1 probe | 152306-152331 | TACGGAGCACATCAGGCCCAAGAACA | 10µM |

| | | | | |
|---|---|---|---|---|
| BILF2 | BILF2F | 138118-138098 | GCAGCGTTCCTAGCAATGAGT | 6 µM |
| | BILF2R | 138051-138069 | TCCATCCCCGGGAGTGTAT | 6 µM |
| | BILF2 probe | 138072-138093 | CTCTCGGATCGAGTTGGGCCGG | 10µM |
| | | | | |
| BNRF1 | BNRF1 F | 3463-3482 | GGAGTTTCCCCCGATTCAAG | 6 µM |
| | BNRF1 R | 166769-166748 | AAAGGTCAAAGAACAAGGCCAA | 6 µM |
| | BNRF1 probe | 3486-3508 | AGGGCGCAAGTTCTCCGGTACCC | 10µM |
| | | | | |
| BVRF2 | BVRF2 F | 136089-136108 | CCACGGCAGTCTACGGTACA | 6 µM |
| | BVRF2 R | 136188-136173 | GCGGCATTGGCGTCAT | 6 µM |
| | BVRF2 probe | 136110-136134 | ACCTTGCGTGGGTCCTGAAGCACTT | 10µM |
| | | | | |
| BLLF1/ GP350 | GP350 F | 77316-77297 | AGAATCTGGGCTGGGACGTT | 6 µM |
| | GP350 R | 77478-77496 | ACATGGAGCCCGGACAAGT | 6 µM |
| | GP350 probe | 77451-77473 | AGCCCACCACAGATTACGGCGGT | 10µM |
| | | | | |
| FU | F1 | 50099-50115 | GGGTGAGGCCACGCTTT | 1µM |
| | U1 R | 55326-55304 | CAGGTCTACTGGCGGTCTATGAT | 1µM |
| | U probe | 55275-55299 | TCCTCTGGAGCCTGACCTGTGATCG | 10µM |
| | | | | |

| | | | | |
|---|---|---|---|---|
| LF1 | LF1 F | 150962-150943 | GACTGACTCAGGGCCACATC | 20x |
| | LF1 R | 151000-151019 | AGAAAGCGGGCCCATGAAGG | custom |
| | LF1 probe | 150977-150991 | ACGCCGCCTCGCCAG | assay |
| | | | | |
| LF2 | LF2 F | 149269-149286 | CCGGACCGTCAGCTTGAG | 20x |
| | LF2 R | 149335-149314 | CAACCCGGTCTTCTACGTCTAC | custom |
| | LF2 PROBE | 149295-149310 | CCGGCTTCCACTCCTG | assay |
| | | | | |
| LF3 | LF3 F | 140769-140753 | AGGGCTGGGTCCTGAGA | 20x |
| | LF3 R | 140683-140707 | ACACGTGATGTAAGTTTAGCCAGTT | custom |
| | LF3 PROBE | 140720-140734 | GACTTTCGGGGCATT | assay |
| | | | | |
| EBER1 | EBER1 F | 6654-6674 | TGCTAGGGAGGAGACGTGTGT | 6 µM |
| | EBER1 R | 6768-6749 | TGACCGAAGACGGCAGAAAG | 6 µM |
| | EBER1 probe | 6710-6736 | AGACAACCACAGACACCGTCCTCACCA | 10µM |
| | | | | |
| EBER2 | EBER2 F | 6994-7012 | AACGCTCAGTGCGGTGCTA | 6 µM |
| | EBER2 R | 7083-7060 | GAATCCTGACTTGCAAATGCTCTA | 6 µM |
| | EBER2 probe | 7014-7034 | CGACCCGAGGTCAAGTCCCGG | 10µM |
| | | | | |
| BART1-3 | BART1-3 F | 149581-149587 | CTCTTCATGTGAGGTCCGGC | 6 µM |

| | | | | |
|---|---|---|---|---|
| | BART3 R | 149645-149626 | TGTGTCCGGTAAACGCCATA | 6 µM |
| | BART3 probe | 149592-149616 | CCACGGAGACTCGGACGTAGCCCTT | 10µM |
| | | | | |
| BART2-3 | BART2-3 F | 146318-146334 | TCCACTTTGTGTTACAGGTCCG | 6 µM |
| | BART3 R | 149645-149626 | TGTGTCCGGTAAACGCCATA | 6 µM |
| | BART3 probe | 149592-149616 | CCACGGAGACTCGGACGTAGCCCTT | 10µM |
| | | | | |
| GAPDH | Spans exons | | Assay ID hs99999905.m1 FAM/TAMRA<br>Applied Biosystems | 20x |
| | | | | |
| PGK1 | Exon 4/5 assay | | Assay ID hs99999906.m1 FAM/TAMRA<br>Applied Biosystems | 20x |
| | | | | |
| B2M | Spans exons | | Assay ID hs00187842 FAM/TAMRA<br>Applied Biosystems | 20x |

* Coordinates taken from accession number NC007605 (Human Herpesvirus 4 type 1, complete genome)